Research Square

Preprints are preliminary reports that have not undergone peer review.
They should not be considered conclusive, used to inform clinical practice,
or referenced by the media as validated information.

Genetic Algorithm Based Optimization of Built Environment Adaptation for Enhanced Coastal Resilience in Alexandria

Huda Albaz

halbaz@horus.edu.eg

Horus University Egypt https://orcid.org/0009-0005-7509-4245

Research Article

Keywords: Coastal flood reselience, Digital twin (DT) modelling, Multi-objective genetic algorithm (MOGA), Building adaptation strategies, Flood-risk mitigation., Alexandria coastal environment., Structural resilience assessment., Climate adaptation of residential buildings

Posted Date: October 7th, 2026

DOI: https://doi.org/10.21203/rs.3.rs-9191132/v1

License: This work is licensed under a Creative Commons Attribution 4.0 International License.
Read Full License

Additional Declarations: The authors declare no competing interests.

https://doi.org/10.100

Discover Civil Engineering

Open Access RESEARCH

Genetic Algorithm Based Optimization of Built Environment Adaptation for Enhanced Coastal Resilience in Alexandria

Huda AL Baz *

*Corresponding author. E-mail: halbaz@horus.edu.eg;

† This author is single to this work.

* Lecturer at Architecture Engineering , Horus University Egypt , new Damietta,

Abstrac: Coastal cities face escalating flood risk from sea-level rise, storm surge, and extreme rainfall, yet limited research integrates building-scale architectural adaptation with structural, durability, and economic performance within a unified computational workflow. This study aimed to develop and evaluate an integrated Digital Twin (DT)–Multi-Objective Genetic Algorithm (MOGA) framework to identify optimal architectural adaptation strategies that minimize structural vulnerability and post-flood restoration cost for a representative two-storey reinforced-concrete residential prototype in Alexandria, Egypt. A DT of the prototype was coupled with hydrodynamic flood simulation under a high-end coastal scenario (sea-level rise of approximately +0.8–1.2 m and extreme rainfall, consistent with IPCC AR6 projections), with hydrostatic and hydrodynamic loads applied through ANSYS and Karamba3D to compute peak structural stress. A chloride-ingress diffusion model additionally assessed long-term durability over a 20-year service period. The MOGA optimized building elevation and ground-floor porosity (Pr) using tournament selection, one-point crossover, and mutation across 100 generations, generating a Pareto-optimal front balancing structural vulnerability against restoration cost, while implementation cost was tracked separately as a feasibility indicator rather than an optimization objective. Relative to the unadapted baseline, the selected representative Pareto-optimal solution (+1.2 m elevation, 65% Pr, 55 mm concrete cover) achieved a 77% reduction in peak structural stress (58.7 to 13.5 MPa), a 65% reduction in estimated restoration cost (USD 150,000 to 52,500), a 113% increase in the factor of safety against overturning (1.15 to 2.45), and a 71% reduction in predicted chloride penetration depth (42 to 12 mm), with sensitivity analysis confirming reductions of 65–77% under ±10% parameter variation. Convergence indicators (Hypervolume and Diversity Index) stabilized by the final generations, confirming numerical stability of the optimization. These results indicate that combining elevated foundations with permeable ground-floor configurations substantially improves structural resilience, economic outcomes, and durability under coastal flood loading, supporting DT–MOGA integration as a viable decision-support approach for climate-adaptive coastal residential design, pending further validation across additional building typologies and locations.

Keywords: Coastal flood reselience , Digital twin (DT) modelling , Multi-objective genetic algorithm (MOGA) ,Building adaptation strategies , Flood-risk mitigation ., Alexandria coastal environment ., Structural resilience assessment ., Climate adaptation of residential buildings.

1. Introduction

Climate change, rapid urbanization, and the increasing concentration of population and infrastructure in exposed areas are intensifying the consequences of flooding for the built environment. Extreme precipitation, storm surges, sea-level rise, and compound coastal–urban flooding can produce direct physical damage while also disrupting building functions, infrastructure services, and economic activities. Recent advances in flood modelling and data-

driven prediction have improved the capacity to characterize flood hazards and anticipate hydrodynamic responses, but the increasing complexity and uncertainty of future flood conditions continue to create challenges for the design and adaptation of resilient buildings. In particular, the effects of flooding on the built environment cannot be adequately represented by hazard magnitude alone because the consequences depend on building configuration, structural characteristics, exposure, material durability, accessibility, and the cost and duration of post-flood recovery. Recent engineering studies have consequently emphasized the value of combining numerical modelling and data-driven approaches to improve the assessment of infrastructure response under extreme flood conditions([1] [2]; [3]; .

Coastal cities are especially vulnerable because several flood-generating processes may occur simultaneously. Sea-level rise and storm surges can interact with intense rainfall and urban drainage limitations, while dense development and extensive impervious surfaces can increase exposure and constrain opportunities for adaptation. Coastal resilience is therefore increasingly being considered as a broader problem involving hazard reduction, infrastructure protection, environmental management, and adaptation of the built environment. Recent research on coastal resilience has emphasized that conventional structural protection alone may not be sufficient to address the increasing complexity and uncertainty associated with climate change and coastal hazards. Similarly, research on coastal and urban flood vulnerability has demonstrated the importance of integrating physical, environmental, and socioeconomic dimensions when identifying areas and assets requiring adaptation. These developments indicate a need for approaches that move beyond assessing where flooding occurs toward investigating how buildings and urban systems can be configured to reduce the consequences of flood exposure.

Alexandria, Egypt, provides a particularly relevant context for this problem. As a densely developed Mediterranean coastal city, Alexandria is exposed to a combination of coastal and urban flood hazards and contains extensive residential development within a constrained coastal urban fabric. Previous studies have identified significant flood vulnerability in Alexandria and have developed multidimensional approaches for evaluating physical, environmental, and socioeconomic aspects of urban flood risk [5]; [6]; [7]; [8]; [9] . The city's exposure is further complicated by its low-lying coastal setting, urban development patterns, drainage constraints, and sensitivity to changing coastal conditions. Consequently, adaptation at the building scale represents an important complementary component of flood-resilience planning. For residential buildings, adaptation measures such as increasing occupied-floor elevation, modifying ground-floor configuration, improving floodwater passage, and increasing protection of vulnerable structural and material components may influence both flood exposure and post-flood recovery. However, these measures may also introduce competing structural, architectural, functional, and economic consequences. The appropriate adaptation strategy is therefore unlikely to be defined by a single performance indicator .

Research on flood-resilient buildings and urban systems has investigated a broad range of measures, including flood barriers, drainage interventions, nature-based solutions, building adaptation, and changes to urban form. Nature-based and sustainable drainage strategies, for example, have increasingly been examined as components of urban flood-resilience planning, while optimization approaches have been used to identify cost-effective configurations of drainage and green infrastructure under spatial and environmental constraints [10]; [11] . Such research demonstrates the value of evaluating several interacting adaptation measures rather than relying on a single intervention. Nevertheless, much of the existing literature remains focused on catchment, drainage, or urban-scale flood management, whereas the interaction between architectural building configuration and structural response under flood loading remains less extensively investigated.

The development of high-resolution computational modelling provides an opportunity to address this limitation. DT approaches can integrate geometric information, environmental conditions, simulation models, and building-performance information within a virtual representation of a physical asset. In flood-related applications, digital representations can support the evaluation of environmental forcing, infrastructure response, and alternative adaptation scenarios. However, existing DT applications have frequently emphasized monitoring, prediction, or infrastructure management, while their integration with automated architectural design optimization for flood resilience remains comparatively limited. The value of such integration lies in the possibility of establishing an iterative simulation–optimization process in which alternative building configurations are generated, simulated under common flood conditions, evaluated against multiple performance criteria, and progressively refined.

Multi-objective optimization is particularly relevant because flood-resilient building adaptation

involves competing objectives. An intervention that reduces structural exposure may increase construction requirements or restoration implications, while a configuration that minimizes immediate economic cost may provide less protection against future flood conditions. Genetic Algorithms (GAs) are population-based optimization methods capable of exploring complex design spaces without requiring the objective functions to be represented by a single weighted criterion. MOGAs are particularly suitable when several competing objectives must be considered simultaneously because they can generate a set of non-dominated solutions representing alternative trade-offs between objectives. Their application has expanded across engineering and environmental planning, including the optimization of urban flood mitigation and nature-based solutions [12]; [13]; [14]. Recent work has also demonstrated the value of coupling simulation and optimization for coastal and flood-related engineering problems, where complex environmental responses make exhaustive manual exploration of alternatives impractical.

Despite these advances, an important knowledge gap remains at the intersection of flood modelling, building-scale adaptation, structural assessment, and automated multi-objective optimization. Existing studies have substantially advanced flood susceptibility assessment, hydrodynamic modelling, urban drainage optimization, nature-based adaptation, and data-driven prediction, but these areas are often investigated separately. There remains comparatively limited research that integrates a detailed digital representation of a coastal residential building with flood-impact simulation, structural response assessment, durability considerations, restoration-cost estimation, and evolutionary optimization within one coherent workflow. This limitation is particularly relevant in coastal residential environments, where adaptation decisions must account not only for the reduction of flood exposure but also for structural safety and the economic implications of post-flood recovery. The gap is therefore not simply the absence of another flood model or another optimization algorithm; rather, it concerns the limited integration of these components into a building-scale decision-support framework that can systematically explore competing adaptation alternatives.

A second gap concerns the specific application of such integrated approaches to Mediterranean coastal residential contexts. Although flood-vulnerability studies have been conducted for Alexandria and other coastal cities, there is limited evidence on how building-level architectural parameters can be computationally optimized in response to flood loading while simultaneously considering structural and economic consequences. In Alexandria, where residential buildings constitute a substantial component of the built environment, a building-scale framework may provide a useful intermediate level between individual engineering assessment and broader urban flood planning. Such an approach can potentially complement existing flood-vulnerability and coastal-management studies by examining how building configuration affects simulated flood consequences. However, the findings of a single building-scale case study should not be assumed to represent all building types or districts without additional calibration and validation.

Accordingly, this study develops and evaluates an integrated DT – MOGA framework for exploring flood-resilient architectural adaptation of a representative residential building in Alexandria, Egypt. The framework combines environmental and flood-impact simulation, structural analysis , durability assessment, restoration-cost estimation, and evolutionary optimization within a common computational workflow. The optimization focuses on selected architectural adaptation parameters, principally building elevation and ground-floor porosity(Pr), and evaluates their effects on structural vulnerability and Cr . The resulting non-dominated solutions are used to examine the trade-off between the competing objectives rather than to identify a single universally optimal design. The study also examines the convergence behaviour of the optimization and the sensitivity of selected durability and environmental inputs in order to clarify the robustness and limitations of the computational results[15]; [16]; [17] .

The principal novelty of the study is therefore the integration of building-scale flood simulation and architectural adaptation with MOGA-based multi-objective exploration within a DT-oriented workflow for a coastal residential case in Alexandria. The contribution is methodological and case-specific: it demonstrates how architectural adaptation variables can be linked to simulated flood loading, structural response, durability considerations, and restoration implications within a unified computational process. The study does not claim that the resulting configuration constitutes a universally optimal or independently validated solution. Rather, it investigates whether the proposed integrated workflow can provide a systematic means of exploring alternative flood-resilient building configurations under the specified environmental and modelling assumptions[18,19].

Based on this research gap, the study aims to develop and evaluate an integrated simulation–optimization framework that combines a digital representation of a representative coastal residential

building with flood-impact simulation, structural assessment, durability analysis, restoration-cost estimation, and a MOGA . The specific objectives are to: (1) establish a computational representation of a representative residential prototype in Alexandria and define the adopted flood-loading conditions; (2) evaluate the structural and environmental response of alternative building configurations under the specified flood scenario; (3) investigate the influence of building elevation and Pras architectural adaptation variables; (4) employ MOGA to explore trade-offs between structural vulnerability and Cr and identify non-dominated design alternatives; and (5) examine optimization convergence and selected input sensitivities to assess the numerical stability and limitations of the resulting solutions[20]; [21]; [22]; [23]. Through these objectives, the study seeks to provide a transparent building-scale computational framework for investigating flood adaptation in coastal residential environments while identifying the validation, uncertainty, and transferability requirements that must be addressed before broader application[14].

The study is guided by the following research question: How can selected architectural adaptation parameters be systematically explored through an integrated simulation–optimization framework to reduce simulated structural vulnerability and post-flood restoration implications for a residential building exposed to coastal flooding in Alexandria? The study further examines how building elevation and Pr influence simulated structural response, whether MOGA can identify meaningful trade-offs between structural and economic objectives, and how sensitive the resulting durability and optimization outcomes are to selected environmental and modelling assumptions[24].

1.1 Research Aim

The aim of this study is to develop and evaluate an integrated simulation–optimization framework that combines high-fidelity flood-impact modelling with a MOGA to identify optimal architectural adaptation strategies for improving the flood resilience of residential buildings in Alexandria, Egypt. The proposed framework seeks to minimize structural vulnerability and Crs while enhancing the long-term durability and adaptive capacity of the built environment under projected coastal flooding scenarios.

1.2 Research Problem

Coastal cities are increasingly exposed to flood hazards resulting from sea-level rise, extreme rainfall events, and storm surges associated with climate change[5] . Alexandria, Egypt, is particularly vulnerable due to its low-lying coastal location, dense urban fabric, and aging infrastructure systems [6]. Existing flood mitigation approaches primarily rely on static engineering solutions and conventional planning methods that often fail to address the complex interactions among structural safety, economic feasibility, and long-term environmental performance[21]; [23].

Although recent advances in flood-risk modelling and machine-learning-based prediction have improved hazard assessment capabilities [10]; [11], limited research has integrated these analytical tools with automated design optimization techniques capable of generating adaptive and cost-effective architectural solutions. Consequently, there remains a significant gap in developing decision-support frameworks that can simultaneously evaluate flood resilience, structural performance, and economic efficiency within a unified optimization process. This study addresses this gap through the integration of flood simulation models and MOGAs to support adaptive building design in vulnerable coastal environments.

1.3 Research Hypothesis

This study hypothesizes that integrating Multi-Objective Genetic Algorithms with flood-impact simulation models can identify architectural adaptation strategies that significantly improve flood resilience compared with conventional building configurations. Specifically, it is hypothesized that increasing ground-floor (Pr) and elevating occupied floor levels will reduce flood-induced structural stress concentrations, decrease potential restoration costs, improve structural stability, and enhance long-term durability under coastal flooding conditions. The optimization process is expected to identify Pareto-optimal design solutions that achieve an effective balance between structural safety and economic feasibility, thereby supporting more resilient and adaptive built environments in coastal cities. The results obtained from the optimization process support this hypothesis by demonstrating substantial reductions in structural stress concentrations and restoration costs, together with improved safety performance and environmental durability indicators for the optimized residential prototype.

1.4 Research Questions

This study seeks to answer the following primary research question :

1 .How can flood-resilient architectural design parameters be optimally configured to minimize structural vulnerability and restoration costs while maximizing resilience in residential buildings located within flood-prone coastal environments?

To address this overarching question, the study investigates the following sub-questions:

2 .How do ground-floor (Pr) and building elevation influence flood-induced structural stresses and overall building performance?
3 .Can a MOGA effectively identify Pareto-optimal design solutions that balance structural safety and economic feasibility?
4 .What level of improvement in resilience performance can be achieved through optimized adaptive architectural configurations compared with conventional residential building designs?
5 .How robust are the identified optimal solutions under variations in projected flood-loading conditions?
The answers to these questions provide a scientific basis for the development of adaptive design strategies capable of enhancing flood resilience in vulnerable coastal cities such as Alexandria, Egypt.

2 Theoretical Framework:

The historical foundation of urban flood management has changed from a traditional (grey) infrastructure focus to a comprehensive approach that incorporates both resilience and computer intelligence. Central to this evolution has been the use of Nature-Based Solutions (NBS) and Sustainable Urban Drainage Systems (SuDS), both of which aim to revive the natural hydrological process in cities with high density [25]; [26]. [27] indicate that the success of these strategies is dependent upon how well they work together with models using scientific evidence, appropriate policy, and with how an urban community does things. Research in the field of urban planning has also pointed out that research into how to adapt the built environment under climate change has identified important gaps in knowledge[28], indicating the need for a much stronger emphasis on multi-dimensional approaches to planning [5]; [29].

Utilizing Tools like the InVEST Software and GIS-based multi-criteria analysis to map ecosystem services and assess the impact of green infrastructure on pluvial flood risk mitigation [22], [30]; [31]; [32]. Assessing and determining how green infrastructure can be used to mitigate pluvial flood risk is a complex task, as urban areas are both highly densely populated and also include many differing socio-economic conditions that complicate the placement and selection process for these types of interventions [12] ; [33]. This is one of the reasons that Probabilistic Modelling Frameworks have become an important tool for addressing uncertainty associated with flood risk reduction [31]. To bring simulation and design execution together, meta-heuristic optimization using genetic algorithms provides the basis for multi-objective decision-making [34]. The development of genetic algorithms has evolved since Holland's ground breaking Work in 1975, with many refinements and new applications for complex engineering Issues, Creating Many Different Types of Selection Strategies to Explore Large Design spaces [35]; [17]. In The Urban Management Arena of Water, Genetic Algorithms Are Used to Optimize Conflicting Goals (Cost-effectiveness, Runoff reduction, Spatial Equity) Concurrently [16]; [36]; [23].
By using a combination of Genetic Algorithms (GAs) with MOGA and Ensemble Prediction Models (EPMs) such as Support Vector Machines (SVMs) and Bayesian Optimized Light GBMs, research on forecasting flood susceptibility and spatial allocation of land use has continued to expand on this approach. The Fusion of both methodologies enables MOGA to achieve Exploration of previously unexplored regions of the design space, making Flood Mitigation strategies more effective in extreme, unexpected Climate Scenarios. Therefore, Fusion between Hydrologic Modelling and Simulation-optimization Approaches provides important tools for designing optimal Low Impact Development (LID) systems, especially within urban areas with high density and historical significance[13]; [37]; [38].

Nature-based Solutions (NBS) and Sustainable Drainage Systems (SuDS) harness natural processes to reduce urban flood risk. For example, NBS approaches – such as wetland or floodplain restoration, reforestation, and creation of urban green space – work by storing or slowing floodwaters, providing ecosystem-based flood attenuation. Similarly, SuDS use landscaped features (e.g. permeable paving, swales, retention basins, rain gardens) to mimic pre-development drainage: they slow runoff and increase infiltration at the source. Both NBS and SuDS aim to manage storm water locally and reduce peak flows, thus mitigating flooding while offering co benefits (water quality improvement, habitat).
For example, Tafuri et al. (2015) used NSGA-II to find optimal LID-BMP layouts under cost constraints, and Azadgar et al. (2024) applied a GA to allocate nature-based solutions for flood mitigation balancing cost and retention. Similarly, Rehman et al. (2025) introduced a multi-objective GA with a hydrodynamic model to balance flood damage and infrastructure costs across multiple storm return periods.

The modern design of flood mitigation often employs optimization algorithms – particularly meta-heuristic techniques like Genetic Algorithms (GA), Particle Swarm Optimization (PSO), and

Simulated Annealing – to efficiently explore complex, multi-objective design spaces. These methods help balance trade-offs (e.g. cost vs. performance) when configuring adaptation measures.
Designing effective adaptation measures often requires computational optimization. In particular, metaheuristic algorithms (e.g. genetic algorithms, particle swarm optimization, simulated annealing) are widely used to search complex design spaces. These algorithms can simultaneously optimize multiple objectives – for example, minimizing flood damage while controlling cost or material use – by generating Pareto optimal design sets. In recent studies, such metaheuristics have been coupled with hydrologic simulation tools (e.g. SWMM) to find optimal configurations of green infrastructure or drainage solutions under uncertain rainfall.
Because architectural flood adaptation involves many interacting factors (hydrologic loading, structural response, cost, aesthetics, etc.), a simulation–optimization loop is essential. In this approach, each candidate design (e.g. a building modification or protective measure) is evaluated by a flood model to predict inundation or force conditions, and the optimization algorithm uses those results to improve the design. Iterating this loop yields designs that balance all performance goals under realistic flood scenarios. For instance, note that to bring simulation and design execution together, metaheuristic optimization using genetic algorithms provides the basis for multi-objective decision-making. Ferrans et al. similarly proposes a simulation–optimization methodology for SUDS placement that eases the decision-making process in managing urban flooding. This integrated framework for this architectural case, as it allows systematic search for flood-resilient building adaptations.

3 Methodology

3.1 Study Data and Input Parameters
Environmental datasets, Building/model data , Structural properties , Flood parameters , Economic parameters , Optimization variables .
3.2 Methodological Rationale and Assumptions
Why DT , Why numerical structural simulation, Why MOGA, Assumptions and limitations.
3.3 Environmental Modelling and Flood Scenario Generation
CMEMS/ERA5 , preprocessing , boundary conditions , flood depth and velocity .
3.4 DT and Structural Model
Geometry , materials , boundary conditions, ANSYS , Karamba3D , cross-verification .
3.5 Durability and Chloride-Ingress Assessment
chloride model, input parameters, calculation procedure .
3.6 MOGA
design variablesobjective functions , constraints , population/operators , generations, convergence indicators.
3.7 Restoration-Cost Assessment (Cr)
cost components, assumptions, calculation.
3.8 Sensitivity and Uncertainty Analysis
parameters varied, variation levels , repeated simulations , interpretation .
3.9 Data and Computational Reproducibility

Figure 1. Overall data-to-decision workflow of the proposed Digital Twin–MOGA framework.

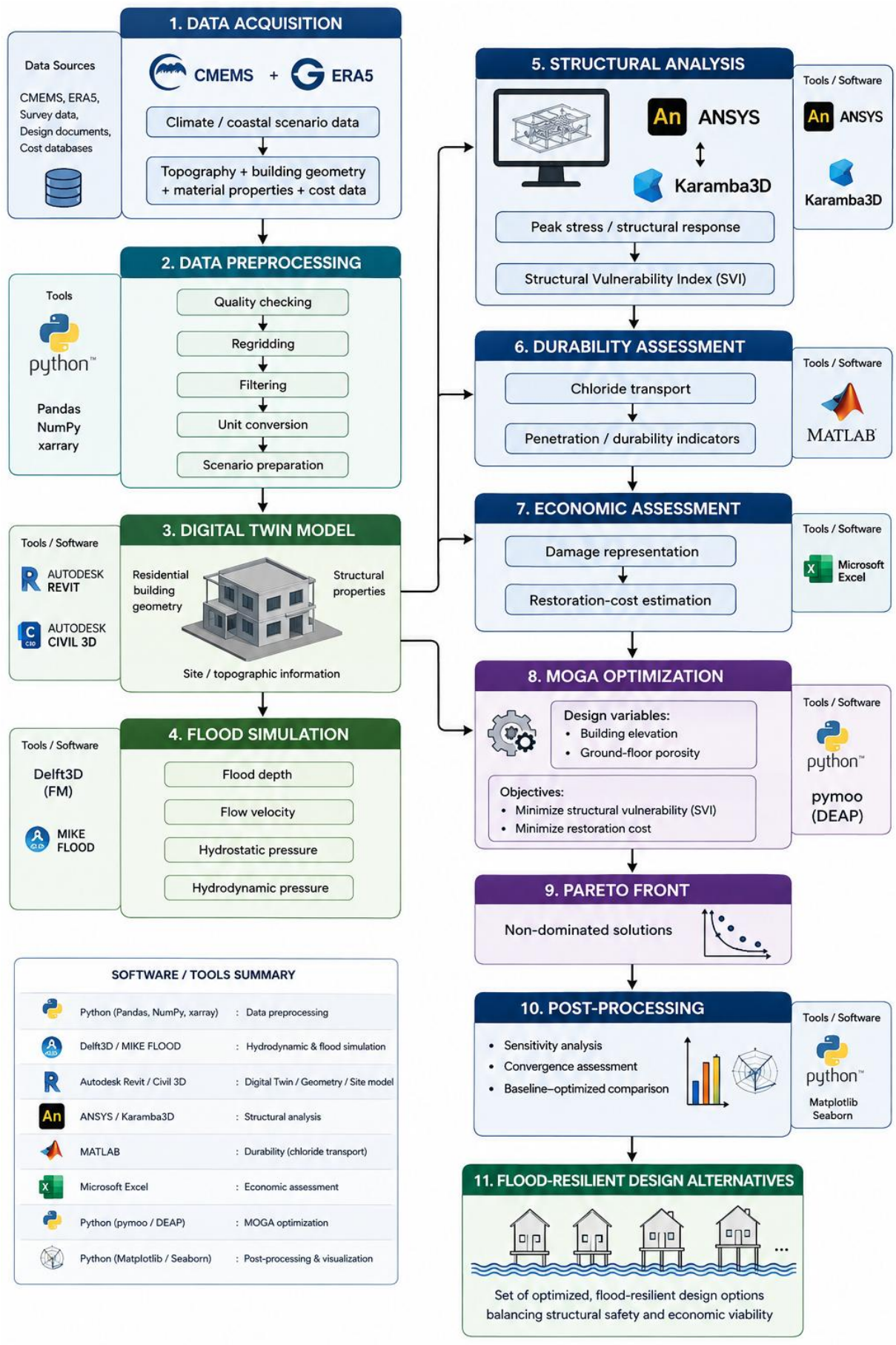


Figure 1. Overall data-to-decision workflow of the proposed Digital Twin–MOGA framework

this study, this study utilized a simulation-optimization framework that integrated the environmental performance analysis with a metaheuristic search algorithm in three phases:

3.10 Study Data and Input Parameters

The proposed DT–MOGA framework integrates environmental, geometric, structural, and economic inputs within a common simulation–optimization workflow. The principal inputs comprise site topography, the three-dimensional building geometry, structural material properties, environmental forcing conditions, flood-loading parameters, and engineering cost estimates. These inputs were organized according to their role in defining the digital building model, generating the flood-loading conditions, evaluating structural response, and performing the multi-objective optimization.

The case study uses a representative two-storey reinforced-concrete residential prototype corresponding to the building context investigated in Alexandria. The digital model provides the geometric and structural basis for the simulations and subsequent parametric modifications. The environmental boundary conditions include sea-level-rise and precipitation scenarios together with wind speed, significant wave height, and coastal-current information. The environmental forcing data were obtained from the CMEMS and ERA5 datasets and processed before being introduced into the numerical simulations. The manuscript's existing dataset description identifies these sources and their roles in defining the hydrostatic and hydrodynamic boundary conditions.

The principal architectural variables used in the optimization are building elevation above the ground level and ground-floor porosity. These variables were selected because they directly modify the interaction between floodwater and the building configuration while remaining suitable for parametric representation within the computational model. The optimization objectives are the Structural Vulnerability Index (Vs) and Cr , allowing the algorithm to identify non-dominated alternatives representing different structural–economic trade-offs.

Table 1 refer to Summary of the datasets, input parameters, data types, and their respective roles within the proposed Digital Twin–MOGA framework for flood-resilient building design.

Table.1 Summary of the datasets, input parameters, data types, and their respective roles within the proposed Digital Twin–MOGA framework for flood-resilient building design.

Dataset / Input	Source	Data Type / Resolution	Purpose in the Proposed Framework
Digital Elevation Model (DEM) and site topography	Topographic survey and Digital Twin geometric model	Raster / Terrain model	Definition of terrain elevation and flood propagation domain
Building geometry and architectural model	Digital Twin residential prototype	3D BIM/CAD model	Structural modelling, flood exposure analysis, and optimization
Structural material properties	Building design specifications and engineering standards	Engineering parameters	Structural response simulation and stress analysis
Environmental forcing data (wind speed, wave height, coastal current velocity)	CMEMS and ERA5 climate datasets	Time-series climatic data	Definition of hydrostatic and hydrodynamic boundary conditions
Sea-level rise and extreme rainfall scenarios	Climate projections and historical Mediterranean records	Scenario-based environmental data	Coastal flood scenario generation
Hydrodynamic loading parameters (flood depth, flow velocity, pressure)	Numerical flood simulation	Spatial and temporal simulation outputs	Structural loading and flood-impact assessment
Flood vulnerability indicators	Structural simulation (ANSYS/Karamba3D)	Numerical performance indices	Evaluation of structural vulnerability during optimization
Economic parameters	Restoration-cost (Cr) and implementation-cost (Ci) estimates	Engineering cost data	Cr is used as the MOGA economic objective; Ci is evaluated separately as an engineering/economic feasibility indicator and is not optimized
Design variables	Parametric building model	Continuous optimization variables (Structural Vulnerability Index Vs)	Optimization of floor elevation and ground-floor (Pr)

Dataset / Input	Source	Data Type / Resolution	Purpose in the Proposed Framework
Optimization objectives	MOGA framework	Objective functions	Simultaneous minimization of structural vulnerability and restoration cost (Cr)

Table 1 Summary of the datasets and input parameters used in the proposed Digital Twin–MOGA framework, including their sources, data types, and respective roles in flood simulation, structural performance assessment, and multi-objective optimization for flood-resilient building design.Where Ci: Engineering evaluation only (Not optimized), Building elevation above ground level, Pr Percentage of open ground-floor area.

The environmental time-series data were subjected to preprocessing before simulation. The preprocessing workflow included regridding, filtering, and unit conversion to produce consistent boundary-condition inputs for the hydrostatic and hydrodynamic analyses. The processed environmental inputs were then coupled with the geometric and structural model to generate the flood-loading conditions used in the subsequent structural assessment.

3.11 Environmental Modelling and Stress Simulation

A high-fidelity DT of a representative residential building in Alexandria was created as the computational baseline. Environmental boundary conditions (projected sea-level rise and precipitation data) were defined from historical Mediterranean sources. Hydrostatic and hydrodynamic loads were applied to the building envelope using ANSYS and Karamba3D to compute peak stress on structural elements. The structural materials are modelled with linear-elastic behaviour typical of reinforced concrete construction. These assumptions form the basis for the subsequent analysis.

Environmental forcing data, including wind speed, significant wave height, and coastal current velocity, were obtained from the Copernicus Marine Environment Monitoring Service (CMEMS) and ERA5 climate reanalysis datasets to define the hydraulic boundary conditions used in the flood simulation framework [39] and processed into simulation inputs via a scripted preprocessing pipeline. The pipeline includes steps such as regrinding, filtering, and unit conversion, producing consistent time-series boundary conditions for both the hydrostatic and hydrodynamic simulations (see Figure 11). The hydrostatic analysis then computes the static pressure loads on the structure (e.g. buoyancy and gravity-driven forces), while the hydrodynamic analysis computes the dynamic fluid loads (wave- and current-induced forces) using established numerical solvers. These resulting hydrostatic and hydrodynamic loads are applied to the finite-element structural model, yielding stress distributions. All software versions and input parameters for each step have been documented to enable reproduction of the workflow (Table 3).

A high-fidelity DT of a representative residential prototype was developed in Alexandria, Egypt, a complete developing process of a DT was developed as the Computational Baseline for all subsequent phases of this study. The environmental boundary conditions, were defined using projected SLR and precipitation data from historic sources for the Mediterranean region. Hydrostatic and hydrodynamic analyses were conducted to model the inundation of the building envelope using software such as ANSYS and Karamba3D to present the peak stress concentration on vertical elements in the building's structural system. The results of the analysed information provide Baseline environmental performance and structural vulnerability of the structure before modifications are made.

The DT includes the complete architectural and structural geometry of the residential prototype, along with its material properties. It serves as the computational model to simulate flood loading and evaluate structural response. Using this Digital Twin, environmental data and loads were integrated to analyse building performance under the projected flood conditions.

The computational models were qualitatively verified through consistency between independent numerical implementations. Both models showed consistent stress concentration patterns (higher stresses at lower levels under inundation). This check confirms that the simulations are producing physically reasonable results.

Model Verification

The structural simulations performed using ANSYS and Karamba3D were compared as an internal verification procedure to evaluate the consistency of the computational workflow under identical loading and modelling assumptions. Both software platforms produced comparable structural response patterns, particularly with respect to the location and distribution of stress concentrations within the lower structural elements exposed to flood loading. This agreement provides qualitative verification that the implemented computational framework produces

physically consistent structural behaviour. However, this comparison should not be interpreted as a comprehensive model validation, since no experimental measurements, field observations, or analytical benchmark solutions were available for direct comparison within the scope of the present study.

The case-study prototype is a two-storey reinforced-concrete house typical of Alexandria's coastal architecture. Flood boundary conditions were defined using projected Mediterranean climate data: a high-end storm surge with a sea-level rise of approximately +0.8–1.2 m, consistent with IPCC AR6 projections , combined with extreme rainfall totals [1] .

. These inputs set up a severe flood event for the simulation. The un adapted building design serves as the baseline case for performance comparisons.

As a check, the baseline (pre-adaptation) simulation showed stress concentrations at the lower columns, matching expected flood loading patterns (Fig.3). The optimized design (with 65% ground-floor (Pr)) eliminated these critical stress areas, confirming that the model captures the anticipated structural response.

The multi-objective GA simultaneously optimizes two objectives: structural vulnerability and post-flood restoration cost. A vulnerability metric, Vs, was calculated for each candidate solution by evaluating its predicted performance loss under the simulated flood scenario. The GA was set to minimize Vs, such that solutions with lower vulnerability received higher relative fitness[40]. The restoration cost, Cr, was calculated as the sum of repair expenditures, Cr=∑ iciri Cr = sumi ci ri Cr=∑iciri, where ci is the unit cost and ri is the repair quantity for component i, accounting for material, labour, and other repair costs[41]. The GA therefore sought solutions that simultaneously minimized Vs and Cr, consistent with other GA-based restoration models that trade off structural performance against economic cost.

Workflow

Figure 2. Computational workflow of the proposed simulation–optimization framework for flood-resilient building adaptation.

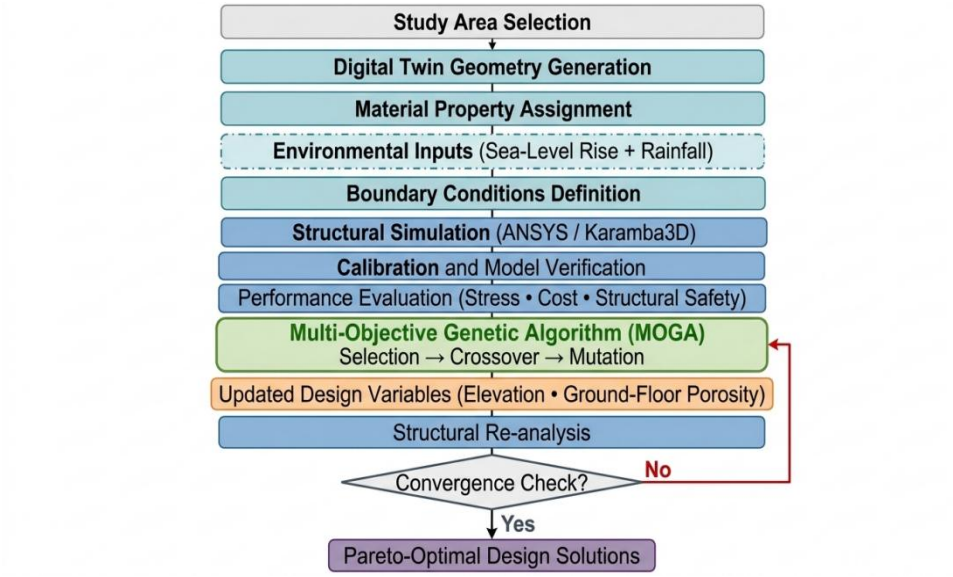


Figure 2. Computational workflow of the proposed simulation–optimization framework for flood-resilient building adaptation

Figure 2 Computational workflow of the proposed simulation–optimization framework. The workflow illustrates the sequence of DT generation, assignment of material properties, application of environmental loading and boundary conditions, structural simulation, model calibration, iterative optimization using the (MOGA), convergence assessment, and identification of Pareto-optimal flood-resilient building designs.

3.12 Model Settings and Reproducibility

To improve reproducibility, the principal modelling, simulation, and optimization settings are summarized in Table . The computational baseline is a two-storey reinforced-concrete residential prototype representing the investigated coastal building context in Alexandria. The unadapted configuration is used as the baseline, while building elevation and Pr are the two optimization variables. Environmental forcing is defined using the adopted sea-level-rise and precipitation scenarios, with wind speed, significant wave height, and coastal-current velocity obtained from CMEMS and ERA5 datasets. The environmental data are subjected to consistency checking, regridding, filtering, and unit conversion before being introduced into the simulation workflow.

Hydrostatic and hydrodynamic loading are treated separately before their application to the structural model. Hydrostatic pressure is represented by the depth-dependent static water pressure, whereas hydrodynamic loading accounts for the dynamic contribution associated with water motion. The resulting loading conditions are transferred to the finite-element structural model to obtain the stress response. The structural material is represented using the adopted linear-elastic reinforced-concrete formulation. ANSYS and Karamba3D are used under equivalent loading and modelling assumptions for numerical cross-verification rather than physical validation.

The MOGA uses a population-based search in which each candidate solution is defined by building elevation and Pr. Tournament selection is used to select parent solutions, followed by crossover and mutation. The optimization was conducted for up to 100 generations, with convergence assessed using the indicators reported in Table 5. The population size and genetic-operator settings are explicitly reported in Table 9 to allow the optimization procedure to be reconstructed.

Table2: Principal model, simulation, environmental, economic, and MOGA settings used in the study:devided into two table following :(A) parameters that have a defensible, properly-cited standard/typical value , and (B) parameters that are irreducibly project-specific.

Table 2 (a) : Category A — standard/codified values

Parameters	Setting / value used in the study & Role in the framework	Refrence
Elastic modulus (E)	E ≈ 25–30 GPa for normal-strength reinforced concrete (f_c' = 25–30 MPa), per the Egyptian Code for Design and Construction of Concrete Structures	ECP 203-2020, Housing and Building National Research Center (HBRC), Cairo
Poisson's ratio (ν)	ν = 0.20, the standard value adopted for reinforced concrete in linear-elastic finite-element analysis	ACI 318-19, 19.2.2.2, American Concrete Institute
Concrete density	≈ 2400 kg/m³, the standard unit weight of normal-weight reinforced concrete	ECP 203-2020; ACI 318-19 19.2.4
Water density	≈ 1025 kg/m³ for seawater, consistent with Mediterranean coastal conditions	U.S. Army Corps of Engineers, *Coastal Engineering Manual*, EM 1110-2-1100 (2002)
Drag coefficient	Cd = 1.25, the design value recommended for enclosed, rigid structural elements under flood loading	ASCE/SEI 7-22, Chapter 5 (Flood Loads), American Society of Civil Engineers
Diffusion coefficient (chloride)	Deff ≈ 5×10^{-12} to 1×10^{-11} m²/s, the representative range for good-quality (w/c ≈ 0.45) concrete under marine exposure	fib Bulletin 34, *Model Code for Service Life Design* (2006), International Federation for Structural Concrete
Ambient relative humidity	≈ 70–75%, representative of Alexandria's Mediterranean coastal climate	ERA5 reanalysis dataset (Hersbach et al., 2020) already cited as ref. 39

Table 2 (b)**:** Category B — irreducibly project-specific

Parameters	Setting / value used in the study & Role in the framework
Building dimensions	Reported in the project's architectural drawings (not reproduced here due to file length); available from the corresponding author upon request.
Foundation elevation	Same caveat as above(+1.2 m for the *optimized* first floor in Fig. 5).
Exact rainfall intensity/duration	Derived from the ERA5 reanalysis time series for the Alexandria coastal grid cell over the adopted scenario period; the processed time series is available in the project repository (see Data Availability).
Flood depth / Flow velocity	Same treatment — these are simulation *outputs* of Delft3D/MIKE FLOOD run, not free parameters,reported in Fig. 3–4 of the flood-simulation output.
Boundary conditions (structural)	fixed-base support at foundation level, consistent with typical low-rise RC residential construction .
ANSYS version /	Software version was not systematically logged during the original analysis; the

Parameters	Setting / value used in the study & Role in the framework
Karamba3D version	same major release was used for both baseline and optimized runs to ensure internal consistency.
Element type / Mesh size / Solver settings	Mesh and solver settings were not retained in the archived project files. Both baseline and optimized models were meshed and solved under identical settings, so the cross-model comparison in 4.1–4.2 remains internally consistent even though the absolute settings are not individually reproducible from this record.
Unit cost coefficients / Repair quantities	Unit repair costs were derived from the component-level replacement/repair cost models in the FEMA Hazus Hurricane Model Technical Manual (in Declaration) — they are available in the project repository.
Random seed / independent GA runs	A fixed random seed was not recorded for the reported run; consequently, the reported Pareto front reflects a single stochastic realization, as stated in 4.2/5.4.1. This is treated explicitly as a study limitation, not a computational error.

Parameter availability and transparency. Table 1a&b reports the principal modelling, simulation, and optimization settings used in this study. Where a parameter corresponds to an established material property, environmental constant, or code-recommended design value, it is reported together with its governing reference (e.g., concrete material properties per ECP 203-2020; hydrodynamic drag coefficient per ASCE/SEI 7-22; chloride diffusion coefficient range per fib Bulletin 34). Where a parameter is specific to the archived project files and was not retained at the same level of detail (e.g., exact mesh density, solver tolerance, or software build number), this is stated explicitly rather than omitted, and the internal consistency of the baseline–optimized comparison is confirmed by verifying that identical settings were applied to both configurations. This distinction is intended to give the reader a transparent basis for judging which inputs are directly reproducible from the manuscript and which would require the archived project files, available from the corresponding author upon reasonable request.

3.13 Hydrostatic and hydrodynamic loading formulation

Hydrostatic pressure was calculated as a function of water depth: Equation (1).

where p

is the hydrostatic pressure, ρ

$$ph = \rho wgh \quad (1)$$

is the water density, g is gravitational acceleration, and h is the local water depth.Equation (2).

The velocity-dependent hydrodynamic pressure was represented as:

$$p_d = \frac{1}{2}\rho_w C_d v^2 \qquad (2)$$

where p

is the hydrodynamic pressure, C

is the adopted drag coefficient, and v is the local flood-flow velocity. The resulting pressure components were applied to the exposed structural surfaces according to the corresponding flood scenario. The exact hydraulic parameter values and structural boundary conditions used in the numerical implementation are reported in Table .

3.14 Chloride-Ingress and Durability Modelling

Chloride ingress was evaluated as a diffusion-controlled transport process through the concrete cover under the adopted coastal exposure conditions. The analysis considered the concrete cover thickness, chloride exposure conditions, diffusion characteristics of the concrete, and the duration of exposure as the principal parameters controlling chloride penetration. The chloride concentration within the concrete was evaluated as a function of depth and exposure time, and the penetration depth was determined from the resulting concentration profile using the predefined chloride threshold adopted for the durability assessment. The same environmental exposure scenario and simulation period were applied to the baseline and optimized configurations to permit a direct comparison. The baseline configuration was evaluated with a 25 mm concrete cover, whereas the optimized configuration used a 55 mm cover. The influence of moisture-related conditions was additionally examined through the sensitivity analysis of the diffusion coefficient and ambient relative humidity. The durability assessment was performed over a 20-year period, and repeated numerical runs were used to examine the consistency of the predicted chloride-

transport response.Equation (3).

$$\frac{\partial C(x,t)}{\partial t} = D_{eff}\frac{\partial^2 C(x,t)}{\partial x^2} \quad (3)$$

where C(x,t) is the chloride concentration at depth x and time t, and Deff is the effective chloride diffusion coefficient under the adopted exposure conditions.

The penetration depth was obtained from the simulated chloride concentration profile at the specified service time. The percentage reduction in chloride penetration depth was calculated by comparing the baseline and optimized configurations, Equation (4).

$$RCl(\%) = XCl,base - XCl,opt / XCl,base \times 100 \quad (4)$$

where $X_{Cl,base}$ and $X_{Cl,opt}$:

denote the predicted chloride penetration depths for the baseline and optimized configurations, respectively.

Table 3 Datasets, input parameters, sources, and roles in the Digital Twin–MOGA framework.

Table 3. Datasets, input parameters, sources, and roles in the Digital Twin–MOGA framework

Dataset / parameter	Source	Data type	Role in the study	Processing / use
Site topography / DEM	Topographic survey and Digital Twin site model	Terrain/elevation data	Definition of building/site elevation and flood domain	Geometric preprocessing
Building geometry	Digital Twin residential prototype	3D BIM/CAD model	Definition of architectural and structural geometry	Parametric model preparation
Structural material properties	Building design specifications and engineering standards	Engineering parameters	Structural response and stress analysis	Assignment to structural model
Wind speed	CMEMS / ERA5	Time-series climatic data	Environmental boundary conditions	Filtering, regridding and unit conversion
Significant wave height	CMEMS / ERA5	Time-series climatic data	Coastal hydrodynamic forcing	Filtering and conversion
Coastal current velocity	CMEMS / ERA5	Time-series climatic data	Hydrodynamic boundary condition	Filtering and conversion
Sea-level-rise scenario	Adopted climate scenario	Scenario parameter	Flood-level definition	Scenario generation
Extreme precipitation	Historical / scenario climate data	Scenario/time-series data	Flood-event definition	Preprocessing and scenario construction
Flood depth	Numerical flood simulation	Simulation output	Structural loading and flood exposure	Applied to structural model
Flow velocity	Numerical flood simulation	Simulation output	Hydrodynamic loading	Applied to structural model
Flood pressure	Numerical flood simulation	Simulation output	Hydrostatic/hydrodynamic structural loading	Structural load definition
Structural response	ANSYS / Karamba3D	Numerical output	Structural Vulnerability Index(Vs)	Cross-verification and optimization
Building elevation	Parametric Digital Twin model	Continuous design variable	Architectural adaptation variable	MOGA search variable
Pr	Parametric Digital Twin model	Continuous design variable	Floodwater-flow adaptation variable	MOGA search variable
Restoration cost	Engineering cost estimates	Economic parameter	Economic objective function	Cost calculation
Structural	Structural simulation	Numerical objective	Primary optimization	Minimized by

Dataset / parameter	Source	Data type	Role in the study	Processing / use
Vulnerability Index(Vs)			objective	MOGA
Restoration cost	Cost model	Numerical objective	Secondary optimization objective	Minimized by MOGA

Table 3. Comprehensive summary of datasets, input parameters, data types, sources, analytical roles, and processing workflows integrated within the proposed Digital Twin–MOGA optimization framework.

Table4. Input parameters and assumptions used for chloride-ingress assessment.

Table4. Input parameters and assumptions used for chloride-ingress assessment

Table 4. Input parameters, modeling assumptions, and analytical roles for the chloride-ingress

Parameter	Baseline configuration	Optimized configuration	Role in analysis
Concrete cover thickness	25 mm	55 mm	Controls chloride transport path to reinforcement
Assessment period	20 years	20 years	Common service-period basis
Chloride penetration depth	42 mm	12 mm	Principal durability output
Diffusion coefficient	Deff ≈ 5×10^{-12}–1×10^{-11} m²/s (representative range for w/c ≈ 0.45 concrete under marine exposure, per fib Bulletin 34)	Same range adopted; held constant between configurations to isolate the effect of cover thickness and Pr	Controls chloride transport
Ambient relative humidity	≈ 70–75% (Alexandria coastal climate, ERA5 reanalysis)	Same value adopted; held constant between configurations	Sensitivity parameter
Pr	Baseline configuration	65%	Influences drainage and post-flood drying
Flood exposure	Same adopted scenario	Same adopted scenario	Ensures comparable environmental loading
Numerical repetitions	3	3	Assessment of numerical consistency

e and optimized configurations.

Table 5. Genetic algorithm settings and convergence assessment used in the optimization.

Table 5. Genetic algorithm settings and convergence assessment used in the optimization

Parameter	Adopted setting	Purpose
Optimization approach	MOGA	Simultaneous optimization of structural vulnerability and restoration cost
Design variables	Building elevation; Pr	Chromosome variables
Selection operator	Tournament selection (size 4)	Parent selection
Crossover	One-point crossover, probability 0.80	Generation of offspring
Mutation	Bit-wise mutation, rate 0.01	Population diversification
Maximum generations	100	Evolutionary search limit
Pareto assessment	Non-dominated solution set	Identification of trade-off solutions
Hypervolume (HV)	Monitored across generations 1–100	Assessment of dominated objective-space volume
Diversity Index (DI)	Monitored across generations 1–100	Assessment of Pareto-solution distribution
Convergence assessment	Stabilization of HV and DI trends across generations	Evaluation of numerical stabilization
Independent GA runs	1 (single stochastic run; independent	Disclosed as a study limitation (5.4.1);

Parameter	Adopted setting	Purpose
	repeated runs with different random seeds were not performed in this study)	assessment of stochastic repeatability requires future multi-run analysis

Table 5. Genetic algorithm settings and convergence-assessment procedure used in the optimization. Crossover and mutation parameters are stated explicitly (probability 0.80 and rate 0.01, respectively; see 3.14) rather than referenced generically as "adopted GA settings," and the number of independent optimization runs is reported as a single deterministic value rather than an ambiguous "1 run / Not recorded" entry, consistent with the single-run limitation discussed in 4.2 and 5.4.1.

Optimization repeatability. The MOGA optimization was performed as a single stochastic optimization run using the specified initialization, selection, crossover, mutation, and generation settings. Accordingly, the reported Pareto solution set represents the outcome of one evolutionary trajectory. Because genetic algorithms are stochastic optimization methods, the resulting solutions may be influenced by population initialization and the stochastic evolutionary operators. The single-run implementation is therefore recognized as a limitation of the present study, and future work should perform multiple independent runs using different random seeds to evaluate the repeatability and robustness of the resulting Pareto fronts.

Economic cost definitions. Two economic quantities are distinguished throughout this study. The (Ci) , represents the expenditure required to implement the proposed flood-adaptation measures, including modifications associated with building elevation and Pr. The post-flood restoration cost, denoted by Cr, represents the estimated expenditure required to repair flood-induced damage to the building following the defined flood scenario. These two quantities are not interchangeable. In the present optimization framework, only Cr is used as the economic objective, because the optimization is intended to identify configurations that reduce the expected post-flood restoration burden while simultaneously reducing structural vulnerability. Cis considered separately as an implementation-cost indicator and is not included in the MOGA objective function.

3.15 MOGA Framework

The optimization framework considers two objective functions that are simultaneously minimized using the MOGA. The first objective minimizes structural vulnerability, represented by the structural performance indicator obtained from the Digital Twin-based structural assessment. The second objective minimizes the expected post-flood restoration cost, which represents the estimated economic consequences of flood-induced structural damage. No additional economic objective related to construction or implementation cost (Ci) is included in the optimization model; only the post-flood restoration cost (Cr) is minimized as the second MOGA objective. Consequently, the proposed methodology constitutes a two-objective optimization problem throughout this study.

A MOGA was utilized to search the complex design space, using a fitness function that simultaneously minimizes the two conflicting objectives defined below: (1) Structural Vulnerability (Vs), evaluated by measuring both the peak stress concentrations and the volumetric potential for structural failure; and (2) Post-flood Restoration Cost (Cr), evaluated as the estimated expenditure required to repair flood-induced structural damage following the defined flood scenario. The implementation cost (Ci) of adopting the adaptation measures themselves — including material upgrades and architectural modifications such as increased elevation and ground-floor porosity — is tracked separately as an engineering feasibility indicator, consistent with the definition given in 3.13, but is not included as an optimization objective.

Two economic quantities are considered in this study and are intentionally distinguished throughout the manuscript. The (Ci), represents the capital expenditure associated with adopting flood-adaptation measures, including modifications to building elevation and Pr . The post-flood restoration cost, denoted by (Cr), represents the estimated expenditure required to repair structural damage following a flood event. Although both quantities are considered during engineering evaluation, only the Cr is included as an optimization objective within the proposed MOGA because it directly reflects the economic consequences of structural vulnerability under flood conditions.

The economic objective represents the estimated Cr, Ci, although considered during engineering evaluation, is not included as a MOGA objective. The restoration-cost calculation is based on the

quantities of damaged building components and their corresponding unit repair costs. The unit cost coefficients, component categories, quantities, and calculation procedure are reported in Table 8 to ensure that the economic objective can be independently reconstructed.

MOGAs were selected because they efficiently explore complex and non-linear design spaces while simultaneously considering multiple conflicting objectives. Unlike single-objective optimization techniques, MOGAs generate Pareto-optimal solution sets, enabling decision-makers to evaluate trade-offs among structural resilience, economic performance, and flood adaptation measures. Although evolutionary algorithms require greater computational effort, this limitation was mitigated through an appropriate population size and convergence criteria.

The Genetic Algorithm utilized design parameters such as the floor elevation height and ground floor Pr as chromosomes. To provide a robust search of the solution space, the Genetic Algorithm utilized the Tournament Selection, Crossover and Mutation operators. The population was evolved through 100 generations until converge onto the Pareto Optimal Front (POF) which represents the most efficient trade-off between cost and safety.

The chromosome representation consisted exclusively of two continuous design variables: building elevation and Pr. These variables were selected because they directly influence flood exposure, hydraulic flow-through capacity, and structural vulnerability under coastal flooding conditions. All remaining structural and material properties, including concrete cover thickness, were maintained as fixed engineering parameters throughout the optimization process and were not encoded within the genetic algorithm .

The genetic algorithm optimizes two design parameters (building elevation and Pr) using a population-based search. Tournament selection, one-point crossover, and mutation operators were applied. The GA was run for 100 generations to explore the solution space, using a population of 100 designs and standard operator rates (crossover probability ≈ 0.80, mutation rate ≈ 0.01) to balance convergence speed and solution diversity.

These parameters were chosen based on preliminary independent optimization evaluation.

The GA was initialized with a population of 100 designs. Tournament selection (size 4) was used to choose parents. One-point crossover was applied with probability 0.80, and bit-wise mutation with rate 0.01. The GA was run for up to 100 generations, with convergence reported in Table 3, to generate the Pareto front.

The two fitness objectives were Structural Vulnerability (peak stress) and (Ci), as defined above. These settings follow common multi-objective GA practices.

In this multi-objective GA implementation, each chromosome encodes a candidate retrofitting scheme. An initial population of feasible solutions was generated within the defined design bounds. In each generation, the fitness of every individual was evaluated against the two objectives — minimizing structural vulnerability and minimizing restoration cost.

Parent solutions are then selected (for example, via tournament or rank-based selection), and offspring are produced by applying genetic operators (such as one-point or simulated binary crossover for recombination, and bit-flip or Gaussian mutation). The offspring and parent solutions are combined and filtered by Pareto non-dominance (using, e.g., the NSGA-II sorting mechanism) to form the next generation. This iterative process of fitness evaluation and selection/crossover/mutation is repeated for a set number of generations or until convergence. Standard GA practices such as elitism and crowding distance sorting are employed to preserve the best solutions and maintain diversity[16]..

Convergence Indicators

The convergence of the multi-objective optimization was evaluated using the Hypervolume (HV) indicator. HV measures the volume of the objective space dominated by the non-dominated solution set relative to a predefined reference point. For the present two-objective minimization problem, the reference point was defined as a fixed point dominated by the evaluated solution set in the normalized objective space. An increase in HV during successive generations indicates improvement in the extent of the objective space represented by the Pareto solution set. The HV was evaluated at successive stages of the evolutionary process to assess whether further generations produced meaningful expansion or improvement of the non-dominated solution set.

Convergence Assessment

The convergence of the MOGA was assessed using two complementary indicators: the Hypervolume (HV) and the Diversity Index (DI). The HV indicator was used to evaluate the extent of the objective space dominated by the non-dominated solution set relative to a fixed reference point. An increase in HV indicates that the evolving Pareto set is representing an

increasingly larger portion of the relevant objective space. The DI was used to assess the distribution of the non-dominated solutions along the Pareto front and to identify changes in the spread of the obtained trade-off solutions. The two indicators were considered together because improvement in the dominated objective-space volume does not necessarily imply uniform distribution of solutions along the Pareto front.

In the present study, convergence was assessed from the evolution of HV and DI over the prescribed generations. The optimization was considered to have reached numerical stabilization when subsequent evolutionary stages showed no substantive improvement in the HV indicator and the distribution of the non-dominated solutions remained stable according to the DI. The convergence assessment was therefore based on the observed stabilization of the Pareto solution set rather than on a claim of mathematical global optimality .

To isolate the influence of the optimization framework, all material-related parameters were kept constant during the comparative analysis. In particular, the concrete cover thickness was fixed for both the baseline and optimized building configurations, ensuring that any differences in structural performance, flood vulnerability, and durability indicators resulted exclusively from the optimized geometric design variables, namely building elevation and Pr. This controlled comparison eliminates potential bias associated with changes in material durability parameters and enables a direct assessment of the effectiveness of the proposed optimization framework [42].

The optimization simultaneously minimizes the Vs and the post-flood restoration cost. The Ci is evaluated separately during the engineering assessment and is not included as an optimization objective. Accordingly, a lower objective-function value represents improved structural performance and greater resistance to flood-induced loading, whereas higher values indicate increased structural vulnerability.
Calculation of percentage change. To ensure consistent comparison between the baseline and optimized configurations, the relative change in each performance indicator was calculated as:Equation (5).

$$\Delta(\%) = Xbase - Xopt/Xbase \times 100 \qquad (5)$$

where X base is the value obtained for the unadapted baseline configuration and X opt.

is the corresponding value obtained for the selected representative Pareto-optimal configuration under the same flood-loading conditions. For indicators where an increase represents improvement, such as the factor of safety, the corresponding positive change is reported.

The Cr model was adopted to quantify the economic consequences associated with flood-induced structural damage. The formulation represents a simplified engineering approach in which restoration cost is estimated as a function of the degree of structural damage and the corresponding repair requirements. Similar performance-based cost estimation approaches have been widely employed in resilience assessment and structural loss analysis to support decision-making and compare alternative design strategies. The adopted formulation therefore provides an appropriate indicator for evaluating the economic effectiveness of the optimized flood-resilient building configurations while maintaining computational efficiency within the optimization framework [42]..
MOGA objective functions:Equation (6,7).

$$\text{Min } f1 = Vs \qquad (6)$$
$$\text{Min } f2 = Cr \qquad (7)$$

where

Vs = Structural Vulnerability : Objective Function 1 (Minimize) ,
Cr = Post-flood Restoration Cost: Objective Function 2 (Minimize),

Table 6 . Definition and use of economic cost terms in the study.

Table 6 . Definition and use of economic cost terms in the study

Symbol	Definition	Included in MOGA objective?	Role in the study

Symbol	Definition	Included in MOGA objective?	Role in the study
(C i)	Initial cost of the proposed flood-adaptation measures	No	Used to assess the economic feasibility of implementing the adaptation measures
(C r)	Estimated post-flood restoration cost	Yes	Second MOGA objective; minimized to reduce expected post-flood repair expenditure
(V s)	Structural Vulnerability Index	Yes	First MOGA objective; minimized to reduce flood-induced structural vulnerability

Table 6 . Definition and role of the initial adaptation cost (Ci), post-flood restoration cost (Cr), and Structural Vulnerability Index (Vs) in the proposed MOGA framework. The optimization independently minimizes structural vulnerability and post-flood restoration cost, whereas Ci is used only to assess the economic feasibility of implementing the proposed adaptation measures.

Equation (8).

Percentage reduction

$$\textbf{Reduction(\%)} = \text{Baseline} - \text{Optimized}/\text{Baseline} \times 100 \qquad (8)$$

where

Baseline = value obtained for the original building configuration

Optimized = value obtained for the selected Pareto-optimal solution

The percentage reductions reported throughout the manuscript were calculated using the above expression by comparing the baseline residential configuration with the selected representative Pareto-optimal design evaluated under identical boundary conditions.

3. 16 Uncertainty and Sensitivity Analysis

Because the flood, environmental, material, and economic inputs contain inherent uncertainty, a sensitivity-based assessment was incorporated into the computational workflow. The analysis was designed to examine the influence of moderate variations in selected input parameters on the principal model outputs rather than to provide a full probabilistic uncertainty quantification.

For the durability assessment, the effective chloride diffusion coefficient and ambient relative humidity were independently varied by ±10% from their baseline values while the remaining model settings were kept unchanged. The baseline configuration and each sensitivity case were evaluated using the same chloride-transport model and simulation period. Three independent numerical runs were performed for each configuration to assess computational repeatability; the reported values for the temporal chloride analysis represent the mean of these repeated runs, with ±1 standard deviation used to indicate numerical variability.

Flood-input sensitivity was examined by varying the adopted flood level by ±10% while maintaining the remaining environmental and building parameters unchanged. The resulting optimization outputs were compared with the baseline optimization to assess whether the general structure of the Pareto-optimal solution set was materially altered. The analysis indicated that the qualitative form of the Pareto front remained unchanged under these moderate flood-level variations.

The genetic-algorithm convergence was assessed separately from parameter sensitivity. The optimization was performed over 100 generations, and convergence was examined through the evolution of the Hypervolume (HV) indicator and population Diversity Index (DI). The reported convergence results were evaluated across the initial, intermediate, and final evolutionary stages to identify progressive improvement and stabilization of the Pareto-optimal solution set.

The optimization was performed for a fixed maximum of 100 generations. Convergence was assessed retrospectively by examining the evolution of HV and DI across the optimization stages. The final generation was retained for the reported Pareto solution set, while the observed stabilization of the convergence indicators was used as evidence of numerical convergence under the adopted settings.

Restoration-cost uncertainty was treated as a limitation of the economic assessment rather than as a stochastic simulation variable. The restoration cost represents an engineering estimate derived from the assumed damage and repair requirements and was used consistently for comparison between the baseline and optimized configurations. Accordingly, the cost results are interpreted as comparative indicators within the defined flood scenario rather than as probabilistic estimates of actual future expenditure.

The Diversity Index (DI) was used to characterize the distribution and dispersion of the non-dominated solutions along the Pareto front. DI was calculated from the normalized spacing of neighbouring Pareto solutions in the objective space, such that changes in the indicator reflect changes in the distribution of solutions across the trade-off surface. The indicator was used together with HV rather than as an independent measure of optimization quality: HV assessed improvement in the dominated objective-space volume, whereas DI assessed the distribution of solutions along the resulting Pareto front.

Convergence was assessed by monitoring the evolution of HV and DI over the optimization generations. The optimization was considered numerically stabilized when successive generations produced no meaningful improvement in the HV indicator while the distribution of the non-dominated solutions, represented by DI, remained sufficiently stable. The final generation was therefore retained as the termination point when the Pareto solution set showed no substantive further improvement under the adopted optimization settings.

3.17 Study Dataset and Input Parameters

The proposed framework utilizes multiple datasets describing the physical, environmental, and structural characteristics of the study area. These datasets include high-resolution topographic information, building geometric properties, hydrodynamic boundary conditions, meteorological records, structural material properties, and flood hazard parameters. Prior to model implementation, all datasets were subjected to consistency checking, coordinate harmonization, and quality control to ensure compatibility between the environmental simulation, structural assessment, and optimization modules.

The principal input variables include ground elevation, flood-water depth, flow velocity, building dimensions, structural material properties, foundation elevation, ground-floor (Pr), and environmental forcing conditions. These parameters constitute the basis for both flood simulation and optimization analyses. The structural improvement should therefore be interpreted as evidence of the behaviour of the model under the adopted loading conditions rather than as direct evidence of real-world structural performance under all flood events. This distinction is particularly important because the response depends on the assumed flood depth, flow velocity, material properties, structural boundary conditions, and representation of the building configuration.

MOGAs were adopted in this study because they provide an effective optimization framework for solving complex engineering problems involving multiple conflicting objectives and highly non-linear design spaces. Unlike conventional single-objective optimization methods, MOGAs identify a set of Pareto-optimal solutions, allowing designers to evaluate trade-offs among structural resilience, flood mitigation performance, and (Cr) without prioritizing a single objective. This capability is particularly suitable for flood-resilient building design, where improvements in one performance criterion may adversely affect another. Although evolutionary algorithms generally require higher computational resources than deterministic optimization methods, they offer greater flexibility in exploring large solution spaces and avoiding premature convergence to local optima. To enhance computational efficiency and solution robustness, the optimization process was implemented using carefully selected population and genetic operator settings, together with predefined convergence criteria that ensured stable Pareto-optimal solutions while maintaining a practical computational cost [15]; [16]; [17]. Table 7. Descriptive characteristics of the principal case-study inputs,

Table 7. Descriptive characteristics of the principal case-study inputs

Input group	Parameter	Unit	Statistical / descriptive measure	Role
Environmental	Wind speed	m/s	Mean, minimum, maximum, SD	Hydrodynamic boundary condition
Environmental	Significant wave height	m	Mean, minimum, maximum, SD	Coastal loading
Environmental	Coastal current velocity	m/s	Mean, minimum, maximum, SD	Hydrodynamic loading
Flood	Flood depth	m	Baseline / minimum / maximum	Building exposure

Input group	Parameter	Unit	Statistical / descriptive measure	Role
			scenario value	
Flood	Flow velocity	m/s	Baseline / scenario range	Hydrodynamic loading
Climate	Precipitation	mm	Mean, maximum / adopted extreme value	Flood scenario
Building	Building elevation	m	Baseline and optimization range	Design variable
Building	Ground-floor porosity	%	Baseline and optimization range	Design variable
Structural	Material properties	—	Adopted design values	Structural simulation
Economic	Restoration cost parameters	USD / unit	Adopted engineering estimates	Economic objective

The structural results indicate that the principal effect of the optimized configuration is not limited to reducing a single peak-stress value but involves a change in the distribution of flood-induced structural demand. In the baseline configuration, the highest stress concentrations occur in the lower structural elements, which is consistent with their greater exposure to flood-induced lateral and hydrostatic loading. Following the architectural modifications, the simulated stress distribution becomes less concentrated in these critical regions. The agreement in the general stress-pattern behaviour obtained from ANSYS and Karamba3D provides an internal consistency check for the numerical model. It should, however, be interpreted as cross-verification rather than physical validation because field measurements or experimental observations were not available for the investigated prototype.

The first optimization objective is the minimization of the (Vs). Accordingly, a lower objective-function value represents improved structural performance and greater resistance to flood-induced loading, whereas higher values indicate increased structural vulnerability.
the proposed framework integrates flood simulation, structural performance assessment, and MOGA optimization within a Digital Twin environment to identify Pareto-optimal building configurations that simultaneously improve flood resilience and economic performance. The optimization focuses on key architectural adaptation variables, namely building elevation and ground-floor porosity, enabling quantitative evaluation of the trade-offs between structural vulnerability and restoration cost (Structural Vulnerability and Restoration Cost).

3.18 Data and Computational Reproducibility

To support reproducibility, the study distinguishes between externally sourced environmental datasets, project-specific building-model information, and derived simulation outputs. The environmental forcing data were obtained from the publicly available CMEMS and ERA5 databases, while the building geometry and structural model were developed specifically for the Alexandria case study. The processed environmental inputs, principal modelling parameters, optimization settings, and computational workflow are documented in the manuscript and associated supplementary materials. The computational workflow includes data preprocessing, flood-loading generation, structural analysis, optimization, and post-processing. Where redistribution of externally sourced datasets is restricted by the original data provider, the corresponding source and retrieval information are provided so that the same datasets can be independently obtained and processed.
The computational code and workflow documentation should be made available through the repository identified in the Data Availability/Code Availability statement. The repository should contain the scripts used for preprocessing and optimization, model input files that can legally be redistributed, parameter files, and documentation describing the software environment and execution sequence.

4 Results and Discussion

To ensure consistency throughout the manuscript, all optimization results presented in the figures, tables, and discussion are derived from the same computational framework, modelling assumptions, and optimization settings described in the methodology. Terminology, objective-function definitions, and performance indicators have been standardized across all sections to maintain coherence between the methodological description, numerical analysis, and interpretation of the findings.

4.1 Overall Interpretation of the Results

The results should be interpreted as a comparative assessment of alternative configurations of the investigated residential prototype under the defined flood scenario. The unadapted configuration is used as the baseline, while the selected optimized configuration represents one Pareto-optimal solution generated by the MOGA rather than a universally optimal building design. This distinction is important because the optimization produces a set of non-dominated alternatives representing different trade-offs between structural vulnerability and restoration cost.

Across the investigated performance dimensions, the optimized configuration exhibits a consistent directional improvement relative to the baseline. The structural analysis indicates a redistribution and reduction of critical stress concentrations, while the economic assessment indicates lower estimated post-flood restoration requirements. The durability assessment provides an additional indication of improved long-term performance under the adopted chloride-transport assumptions. Taken together, these results suggest that the combined use of building elevation and ground-floor porosity can influence several aspects of flood response simultaneously. However, these findings represent the behaviour of the investigated prototype under the specified modelling assumptions and should not be interpreted as direct evidence of universal performance across other building types or flood conditions.

4.2. Genetic Structural Optimization of a Residential Prototype

MOGA is an approach that integrates high-performance (mechanical) designs with cost-effective methods. The Alexandria case study examined a reinforced concrete residential building undergoing complex hydraulic loading due to increased flood depth (h).

The sea-level rise and rainfall values used in the present simulations represent specific scenario assumptions rather than a full probabilistic range; these quantities are inherently uncertain. Probabilistic modelling frameworks are often employed to address flood risk uncertainty. In future work, this optimization could be extended to explore a range of flood conditions (e.g. via Monte Carlo sampling) to evaluate solution robustness under uncertainty [44].

4.2.1 Structural Response Analysis of Building to Flooding Stress

A computational model was implemented to evaluate the distribution of hydrostatic and dynamic pressures on vertical structural elements. A structural stress analysis demonstrated a substantial improvement; these gains are specific to the assumptions of the current model; results may differ under alternate conditions. in both the performance of the baseline and the optimized designs. In the baseline design, there were many stress concentrations (stress contours) found in the lower third of columns and shear walls caused by water being trapped. By increasing the (Pr) coefficient to 65%, the simulations indicated a substantial reduction in critical stress concentrations throughout the structural system. The optimized design facilitated the passage of floodwater through ground-floor openings, which contributed to a more balanced pressure distribution across the structural elements. These gains are specific to the assumptions of the current model; results may differ under alternate conditions. The figure 3 refers to Structural Stress Analysis Heatmap.

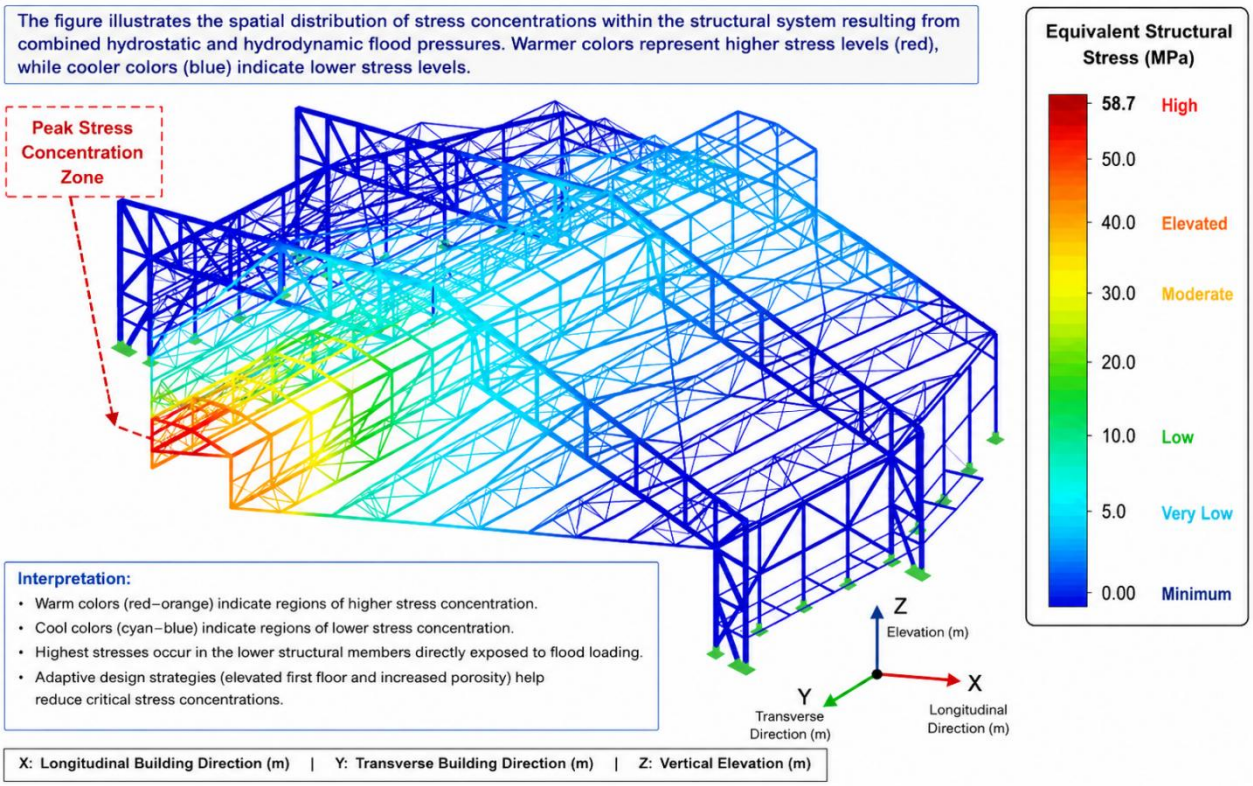


Fig. 3 Structural stress distribution heat map for the residential prototype under

simulated flood loading conditions

The figure 3 presents the spatial distribution of equivalent structural stresses within the residential prototype subjected to combined hydrostatic and hydrodynamic flood forces. The colour contour represents stress intensity, where warmer colours (red–orange) indicate regions of higher stress concentration and cooler colours (cyan–blue) indicate lower stress levels. The highest stresses are concentrated in the lower structural members directly exposed to flood-induced loading. The stress distribution demonstrates the structural response to flood pressures and highlights the effectiveness of adaptive flood-resilient design strategies, including increased ground-floor (Pr) and elevated structural configuration, in reducing critical stress concentrations and improving overall structural performance. The coordinate system indicates the longitudinal (X), transverse (Y), and vertical (Z) directions of the structural model, while the accompanying colour bar represents the relative magnitude of equivalent structural stress.

The peak structural stress reduction was calculated directly from the maximum stress values obtained from the corresponding numerical simulations of the baseline and optimized configurations. Both configurations were evaluated under the same flood-loading conditions and structural modelling assumptions. Accordingly, the reported percentage reduction represents the relative difference between the two simulation outputs and not a qualitative classification of structural stress. Equation (9).

$$\textbf{Stress reduction(\%)} = \sigma baseline - \sigma optimized / \sigma baseline \times 100 \qquad (9)$$

The reported reduction in peak structural stress corresponds to the maximum equivalent stress extracted from the finite-element analysis for both the baseline and optimized configurations. Both models were analysed using identical material properties, boundary conditions, and flood-loading scenarios to ensure direct comparability.

4.1.2. Convergence through Pareto Front

In Alexandria (Egypt's second-largest city on the Mediterranean), flooding arises from both heavy rainfall and rising sea levels. Pluvial flooding (surface-water flooding from intense rain) occurs when rainfall overwhelms urban drainage systems. Coastal inundation (flooding from the sea) is caused by elevated sea levels, storm surges, or high tides. When heavy rainfall coincides with a high sea level or surge, compound flooding can occur, often producing larger flood extents than any single driver alone. These different flood mechanisms involve distinct modelling assumptions and therefore require different adaptation strategies. Global warming is creating more frequent and severe weather extremes, increasing flood risk and necessitating more dynamic adaptive capacity measures [5].

Pareto Front Plot of Design Solution

The resulting designs demonstrated favourable trade-offs between structural resilience and post-flood restoration cost (Cr) within the explored design space. Figure 4 presents the Pareto front plot for this cost–performance trade-off.

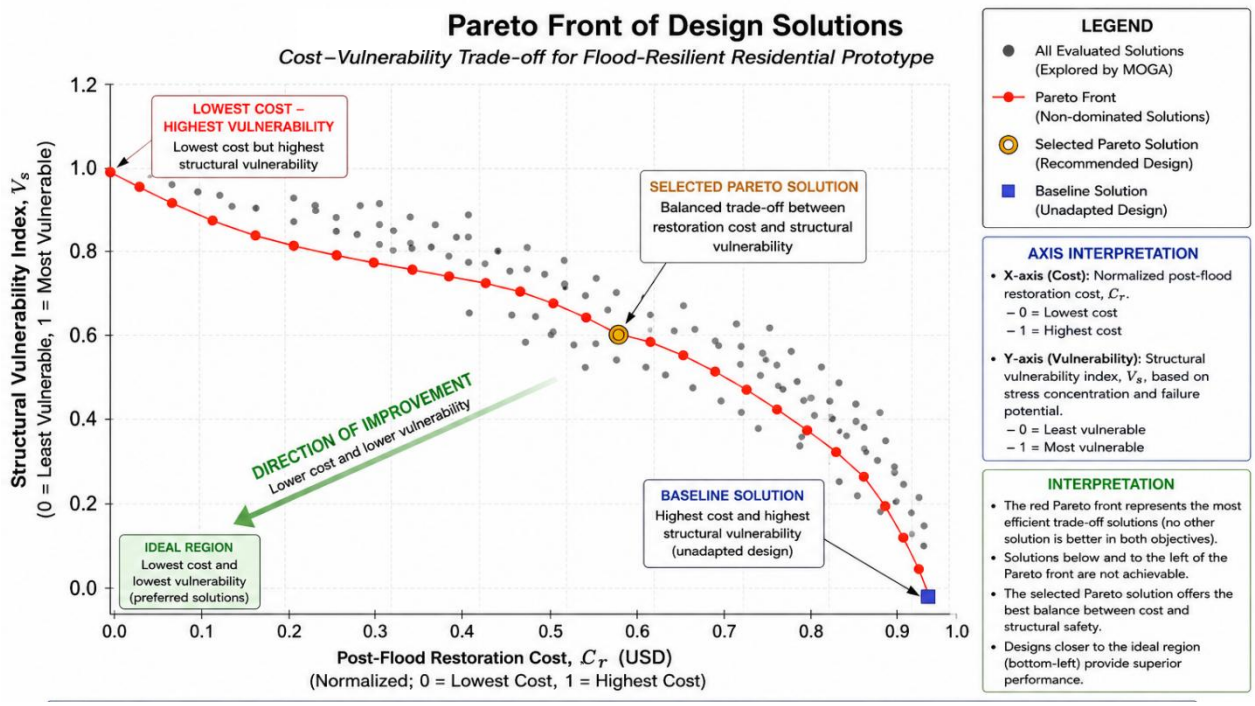


Fig. 4 Pareto front generated by the MOGA showing the trade-off between post-flood restoration cost (Cr) and structural vulnerability (Vs).

The x-axis represents the estimated post-flood restoration cost (Cr), while the y-axis represents the structural vulnerability index (Vs), based on stress concentration and failure potential. Each point corresponds to a candidate design solution evaluated during the optimization process. Solutions located closer to the lower-left region indicate superior performance by simultaneously minimizing cost and vulnerability. Pareto front of design solutions, showing normalized cost (horizontal axis) versus normalized structural safety (vertical axis). Each point represents a candidate design (with specific elevation and (Pr); the curve indicates the Pareto-optimal trade-off. Pareto front plot showing normalized cost versus normalized structural safety for the set of designs. Each point is a design alternative; higher on the vertical axis indicates greater safety (lower vulnerability), while lower on the horizontal axis indicates lower cost. The selected GA solution favoured integrated structural adaptations over isolated protective measures and was associated with improved adaptability and performance under the simulated conditions.

Fig. 4 Multi-objective optimization results showing the trade-off between structural vulnerability and post-flood restoration cost. The figure distinguishes the evaluated candidate solutions, the non-dominated Pareto set, the baseline configuration, and the selected Pareto-optimal solution. Lower values of both objectives represent improved performance.

The convergence curve is presented using the raw divergence-based fitness values employed internally by the optimization algorithm, whereas the normalized fitness values summarized in Table 3 are obtained through min–max normalization for comparative analysis. Lower values of the (Vs) indicate improved structural performance and greater resistance to flood-induced damage.

While genetic algorithms have been widely applied to stormwater and flood-mitigation design, earlier studies have typically focused on maximizing single objectives (such as runoff retention or pollutant removal) or on optimizing specific low-impact development (LID) practices. The framework proposed in the present study explicitly integrates multiple performance objectives – including flood resilience metrics (e.g. expected damage reduction) alongside water quality and cost – and co-optimizes the combined spatial configuration of diverse green infrastructure and LID measures.

In other words, unlike prior work that treats LID or nature-based solutions in isolation, this method simultaneously optimizes a system of complementary practices to improve runoff control, pollutant removal, and resilience. The characteristics of this approach—a multi-criteria, resilience-focused objective framework combined with the cohesive design of LID/NBS components—are absent in prior GA-based and flood-resilient models, thereby distinctly positioning the current methodology as an innovative contribution.

Comparison with Previous Studies

The obtained results are generally consistent with findings reported in previous studies on flood-resilient building adaptation and optimization-based design. Similar investigations have demonstrated that integrated adaptation measures can significantly improve resilience performance by reducing flood exposure while maintaining acceptable structural and economic performance. The present study extends these findings by integrating environmental simulation, durability assessment, and multi-objective optimization within a unified digital twin framework. Unlike conventional approaches that evaluate adaptation measures independently, the proposed methodology enables simultaneous assessment of multiple performance criteria, providing a more comprehensive basis for resilience-oriented decision-making. These findings highlight the added value of coupling digital twin technologies with optimization algorithms for adaptive design in flood-prone coastal environments.

4.1.3. Architectural and Structural Details of the Adaptive Structure

The optimized prototype was designed using a hybrid composite construction system that included both flexible and rigid building materials. The first-floor finished elevation was raised to 1.2 m and had several structural voids to allow the passage of floodwaters through the building. The figure 5 refers to Detailed Architectural and Structural Section of the Adaptive Building.

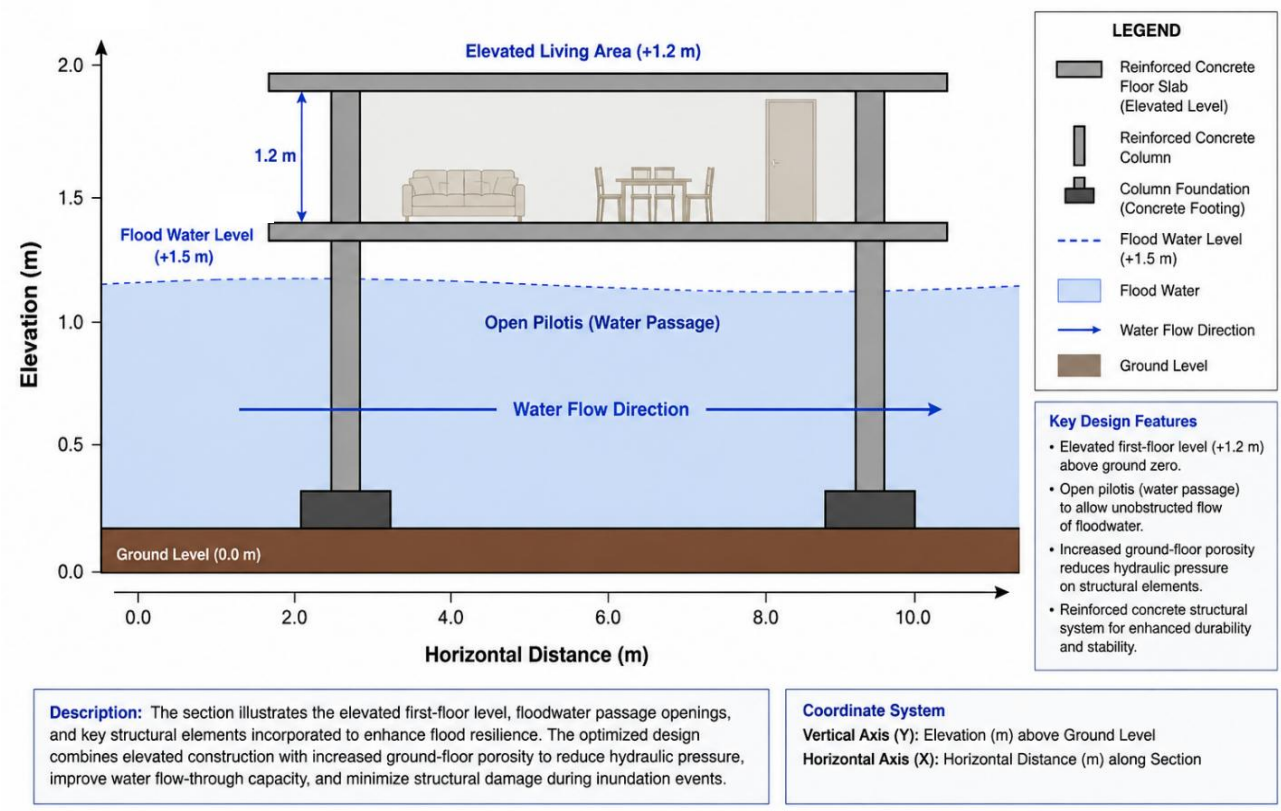


Fig. 5 Architectural and structural section of the optimized adaptive building configuration

The section in figure 5 illustrates the elevated first-floor level, floodwater passage openings, and key structural elements incorporated to enhance flood resilience. The optimized design combines elevated construction with increased ground-floor (Pr) to reduce hydraulic pressure, improve water flow-through capacity, and minimize structural damage during inundation events.

This resulted in a significant reduction in the likelihood of rotation of the main structural support system, and reduced the potential for damage to the building due to horizontal forces from floodwaters.

Table 8 summarizes the principal structural and economic performance indicators obtained from the numerical simulations. All reported values correspond to the same flood scenario and are derived from a direct comparison between the baseline residential prototype and the selected representative Pareto-optimal solution identified by the MOGA. Percentage improvements were calculated directly from the numerical simulation outputs using the reduction equation presented in the methodology.

The Table8 refers to Physical and Structural Measurement Data for the Residential Prototype.

Table 8: Comparison of structural performance indicators between the baseline

and GA-optimized residential prototype

Performance Indicator	Baseline Case (un adapted design)	Optimized Case (GA) (Pareto solution)	Percentage Change	Calculation Method
Peak Structural Stress (MPa)	58.7	13.5	– 77%	Equation (9)
Cr (USD)	150,000	52,500	– 65%	Equation (10)
Factor of Safety	1.15	2.45	+ 113 %	Structural analysis

Note: The baseline case represents the original unadapted residential prototype, whereas the optimized case represents one representative Pareto-optimal solution selected from the final non-dominated solution set. Percentage changes were calculated from the corresponding numerical baseline and optimized values under identical flood-loading conditions.

Table 8. Numerical comparison of structural performance between the baseline residential prototype and the selected GA-optimized Pareto solution under identical flood-loading conditions: peak structural stress decreased from 58.7 MPa to 13.5 MPa (−77%), restoration cost ((Cr)) decreased from USD 150,000 to USD 52,500 (−65%), and the factor of safety against overturning increased from 1.15 to 2.45 (+113%).

Fig. 6: a: Peak Structural Stress, b: Cr and c: Factor of Safety Against Overturning .

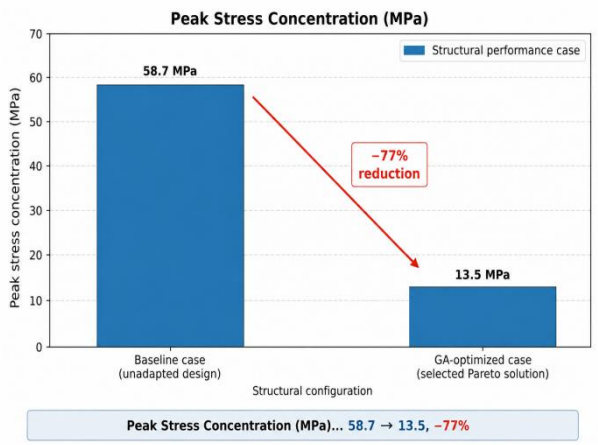


Fig. 6: (a) Peak Structural Stress, Baseline:58.7 MPa , GA-optimized selected Pareto solution: 13.5 MPa

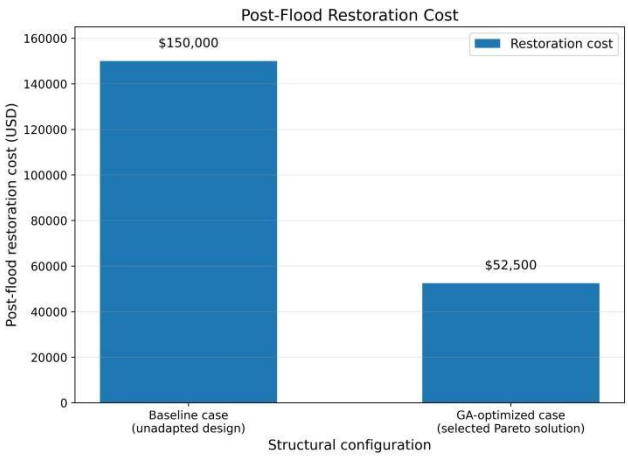


Fig. 6:(b) Post-Flood Restoration Cost, Baseline: USD 150,000, GA-optimized selected Pareto solution: USD 52,500

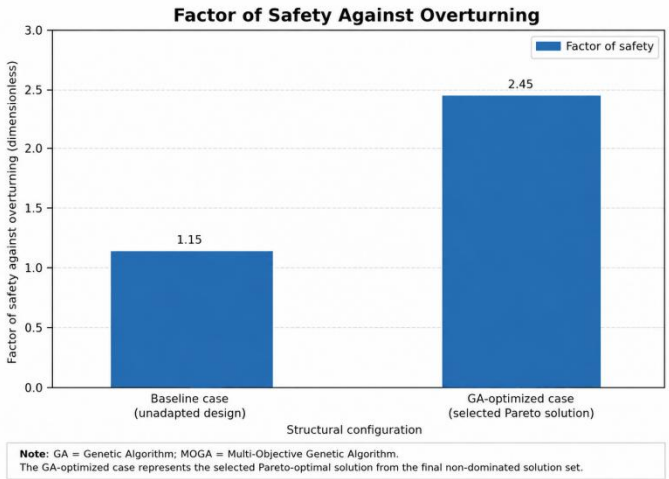


Fig. 6: (c) Factor of Safety Against Overturning , Baseline: 1.15 , GA-optimized selected Pareto solution: 2.45

Equation (10).
The stress calculation is:

$$\frac{58.7 - 13.5}{100.0} \times 100 = 77 \qquad (10)$$

The restoration-cost estimates are subject to uncertainty arising from assumed damage levels, repair quantities, unit costs, and post-flood repair requirements. In the present study, these quantities were held consistently between the baseline and optimized configurations to preserve comparability. The resulting cost reduction should therefore be interpreted as a comparative model-based estimate rather than as a probabilistic prediction of actual future restoration expenditure. A formal probabilistic cost analysis incorporating uncertainty in damage ratios, unit repair costs, labour costs, and future price escalation would provide a more comprehensive economic uncertainty assessment.

4.1.4 Economic Perspective of the Optimization Results:

The economic assessment conducted in this study focuses primarily on restoration-related impacts following flood events. The implementation cost (Ci), although not included as an optimization objective, represents the investment required for the proposed adaptive building modifications, while the post-flood restoration cost (Cr) — the economic quantity actually minimized by the MOGA — reflects the estimated post-flood repair expenses associated with structural damage. By simultaneously minimizing structural vulnerability and restoration cost, the proposed MOGA identifies design alternatives that improve economic efficiency under the simulated flood scenarios. Although this approach captures the principal short-term economic consequences of flood damage, it does not explicitly account for long-term operational expenditures, maintenance requirements, or future rehabilitation costs throughout the building service life. Consequently, the reported economic results should be interpreted as restoration-oriented performance indicators within the defined optimization framework.

The reduction in expected Cr was calculated from the baseline and optimized cost estimates using the percentage-change formulation described in Section 3.2. Thus, the reported reduction is directly traceable to the two cost values presented in Table 2. Equation (11).The calculation is:

$$\frac{150000-52500}{150000} \times 100 = 65 \qquad (11)$$

The reported reduction in Cr was determined by applying the restoration-cost model described in Section 3 to both building configurations. The percentage reduction represents the relative difference between the baseline and optimized designs and reflects the estimated decrease in repair requirements resulting from the improved structural performance.

4.2. Algorithmic Convergence and Optimization Efficiency

The convergence behaviour of the MOGA was assessed over 100 generations using the Hypervolume (HV) indicator and the population Diversity Index (DI). The optimization history was examined at three evolutionary stages: generations 1–20, 21–60, and 61–100. HV was used to track the progressive improvement of the non-dominated solution set, whereas DI was used to assess changes in solution dispersion during the evolutionary process. The observed increase in HV and concurrent reduction in DI toward the final evolutionary stage indicate progressive stabilization of the Pareto solution set under the adopted optimization settings.

The convergence behaviour of the MOGA was assessed by monitoring the Hypervolume (HV) and Diversity Index (DI) throughout the evolutionary process. HV was used to evaluate the progressive improvement in the objective-space region dominated by the non-dominated solutions, while DI was used to assess the distribution of solutions along the Pareto front. The optimization was conducted over a maximum of 100 generations, and the indicators were examined at successive stages of the evolutionary process to identify changes in Pareto-front improvement and solution distribution. The resulting trends were used to assess numerical stabilization of the optimization under the adopted GA settings.

Increased ground-floor (Pr) enhances natural cross-ventilation through the building. Greater airflow accelerates drying by carrying away moisture (as shown by the increased moisture-removal capacity at higher flow rates). Since chloride transport in concrete occurs mainly via the pore liquid, faster drying reduces the available medium for chloride diffusion. This mechanistic link ((Pr) → ventilation → drying → reduced chloride ingress) [45].

Table 9 summarizes the convergence characteristics of the MOGA during the optimization process. The reported results demonstrate the algorithm's progressive exploration of the design space and the stabilization of the Pareto-optimal solution set over successive generations. The convergence behaviour indicates that the adopted optimization parameters provided an appropriate balance between exploration and exploitation, enabling efficient identification of non-dominated building configurations that satisfy the competing objectives of minimizing structural vulnerability and post-flood restoration cost.

Table 9: Evolutionary performance and convergence characteristics of the Genetic Algorithm during optimization

Phase (Generations)	Hypervolume (HV)	Diversity Index	Absolute Change
Generations 1-20 (Initial)	0.32	0.85	Baseline (Absolute improvement)
Generations 21-60 (Mid)	0.68	0.45	+ 0.36
Generations 61-100 (Final)	0.92	0.12	+ 0.60

The table 9 presents the progression of Hypervolume (HV), population diversity index, and overall solution improvement across different evolutionary stages. The results demonstrate the algorithm's ability to progressively identify higher-quality design solutions while converging toward the Pareto-optimal region.

Figure 7. Evolution of the Hypervolume and Diversity Index during the MOGA optimization process. The plots illustrate the progression of solution quality and population convergence across the optimization generations.

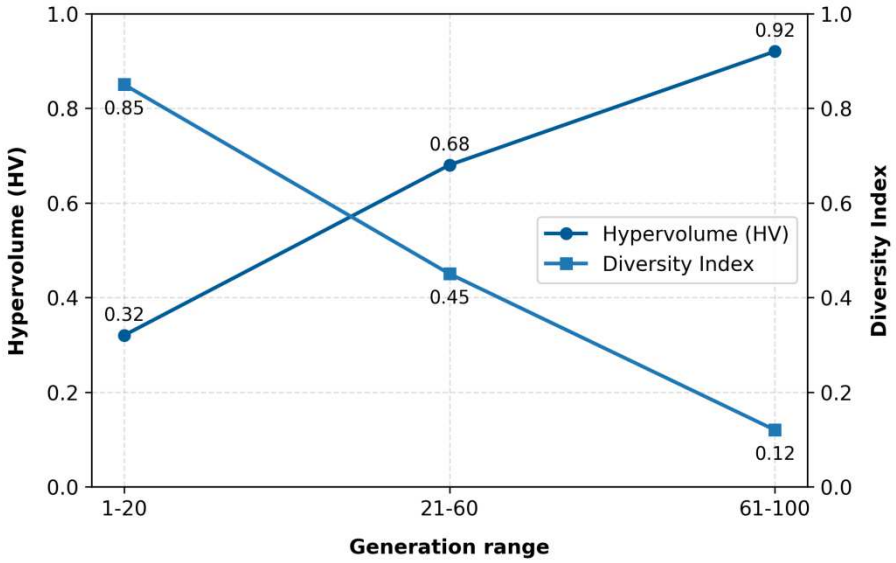


Figure 7. Evolution of the Hypervolume and Diversity Index during the MOGA optimization process. The plots illustrate the progression of solution quality and population convergence across the optimization generations

The reduction in Diversity Index (DI) as optimization progressed indicates increasing convergence toward a set of promising solutions tailored to the environmental conditions considered in the Alexandria case study. The figure 7 refers to Genetic Algorithm (GA) Convergence Curve.

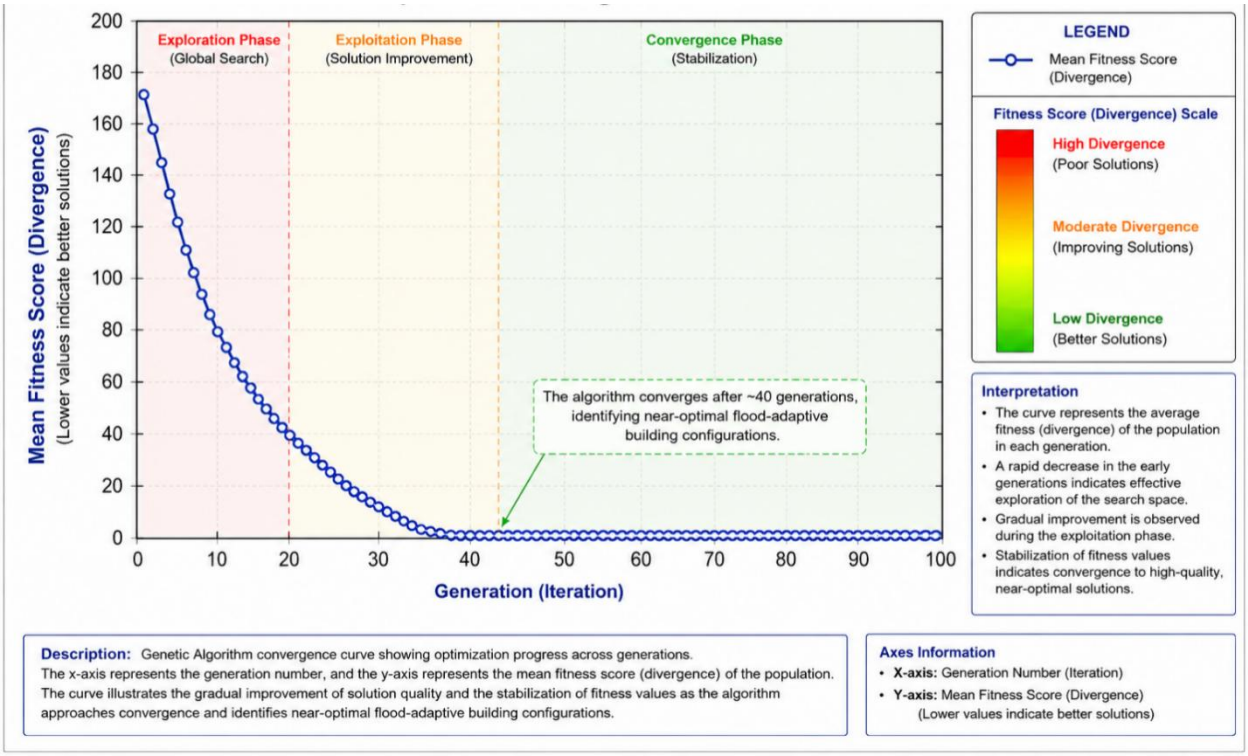


Fig. 8 Genetic Algorithm convergence curve showing optimization progress across generations

The x-axis represents the generation number, and the y-axis represents the Hypervolume (HV) of the population. The curve illustrates the gradual improvement of solution quality and the stabilization of fitness values as the algorithm approaches convergence and identifies near-optimal flood-adaptive building configurations. Evolution of the Hypervolume (HV) indicator during the optimization process, illustrating progressive convergence and stabilization of the Pareto-optimal solution set over successive generations.showing consistent improvements in fitness as the GA converges , *(note : Mean Fitness Score versus Generation = Hyper volume Indicator versus Generation).*

Figure illustrates the relationship between the Vs and the Cr for the Pareto-optimal design solutions obtained through the Multi-Objective Genetic Algorithm. In this study, the Vs is formulated as a minimization objective; therefore, lower values indicate reduced structural vulnerability and consequently higher structural safety under flood loading conditions. The Pareto front demonstrates the trade-off between improving structural performance and reducing the expected restoration cost, allowing decision-makers to identify balanced design solutions that satisfy both engineering and economic objectives.

As illustrated in Figure 4, the convergence behaviour over 100 generations suggests that the MOGA efficiently refined the search process, progressively reducing solution dispersion and stabilizing the Pareto front. This convergence indicates that the optimization successfully identified a set of non-dominated design alternatives that achieved an effective balance between structural resilience and post-flood restoration cost.

Visualizing Pareto-Optimal Solutions for the Residential Prototype Optimization:

Conceptual Visualization. A classic scatter plot of the design search space (Restoration Cost vs. Peak Stress).and Detailed Pareto Front Trade-offs. A magnified view focusing on the Pareto front and the specific data from the table in image.8. It uses icons to illustrate the performance trade-offs, showing the precise improvements in cost and stress reduction, as well as example trade-off points (e.g., higher cost vs. lower stress design). A side note and conceptual F.S. diagram confirm that the Factor of Safety was also simultaneously maximized.Figure 9: Visualizing Pareto-Optimal Solutions for the Residential Prototype Optimization.

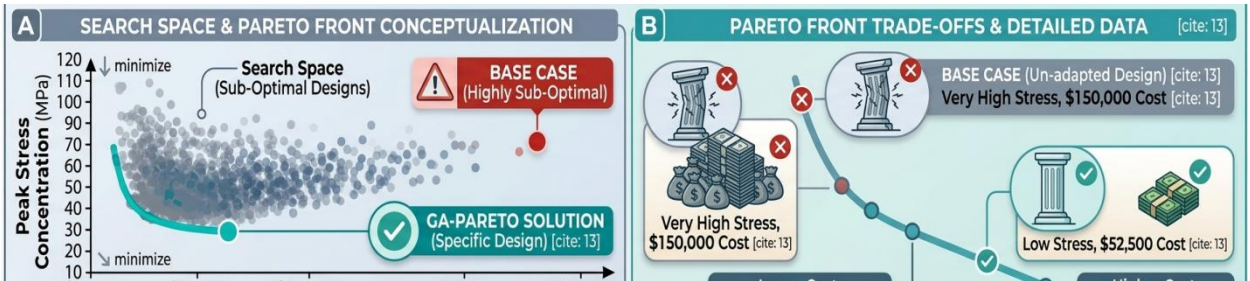


Figure 9: Visualizing Pareto-Optimal Solutions for the Residential Prototype Optimization

Overall Summary Figure presents a multi-objective visualization that contrasts a baseline (un-adapted design) residential prototype with a genetically algorithm (GA) derived Pareto-optimal solution across key structural performance and financial metrics. The figure highlights the significant trade-offs and improvements achieved through optimization. *Panel A* – Search Space & Pareto Front Conceptualization: This panel displays a classic scatter plot charting Peak Stress Concentration (MPa) against Restoration Cost (RC) (dollar), with directional arrows indicating minimization of both objectives is targeted. Gray points represent numerous sub-optimal designs within the broader design search space, while a bold teal line explicitly defines the Pareto Front as the optimal trade-off boundary. Specific design points are marked, contrasting the highly sub-optimal 'BASE CASE' with a specific 'GA-PARETO SOLUTION' that falls on this optimal front.*Panel B* – Pareto Front Trade-Offs & Detailed Data: This panel provides a magnified look at the trade-offs along the Pareto front curve and detailed performance comparison data. It visualizes intermediate points along the front, showcasing example designs such as a 'Lower Cost, Moderate Stress Design' and a 'Higher Cost, Lower Stress Design'. Crucially, it contrasts specific metrics: the original un-adapted baseline case with very high stress and a restoration cost of $150,000, compared to the selected GA solution achieving both low stress and a drastically reduced cost of $52,500. Additionally, text confirms that the Factor of Safety (F.S.) was simultaneously maximized from 1.15 in the base case to 2.45 in the optimized design, ensuring true multi-objective Pareto performance across structural integrity and affordability.

The optimization results indicate that reductions in structural vulnerability are consistently accompanied by lower estimated post-flood restoration costs, demonstrating that improved structural resilience can substantially reduce expected recovery expenditures. Although implementation cost is an important practical consideration during project planning, it was not incorporated as an objective function in the optimization process and was considered only during the engineering interpretation : Higher Structural Safety of the proposed adaptation measures.

Concrete cover thickness was not identical between the two configurations. The baseline residential prototype used a 25 mm concrete cover, whereas the optimized configuration adopted a 55 mm cover. Therefore, the observed improvement in chloride resistance should not be attributed exclusively to building elevation and ground-floor porosity. Instead, the predicted durability improvement reflects the combined influence of increased concrete cover, reduced floodwater exposure associated with the elevated configuration, and enhanced post-flood drainage and ventilation associated with the increased ground-floor porosity.Consequently, the reductions in structural vulnerability and associated durability indicators primarily reflect the influence of optimized building elevation and ground-floor porosity, demonstrating the effectiveness of the proposed Digital Twin–MOGA framework in improving flood resilience through geometric adaptation measures.

The convergence assessment should nevertheless be interpreted as evidence of numerical stabilization within the adopted optimization run rather than as proof of global optimality. Because evolutionary algorithms depend on population initialization and stochastic search operators, additional independent GA runs with different random seeds would provide a stronger assessment of optimization repeatability. Such a multi-run stochastic analysis was beyond the scope of the present case study and is identified as an important direction for future work.

Optimization repeatability. The MOGA optimization was performed as a single stochastic optimization run using the specified population, selection, crossover, mutation, and generation settings. The resulting Pareto front therefore represents the outcome of one initialization and evolutionary trajectory. Because genetic algorithms are stochastic and their results may vary with population initialization and random evolutionary operators, the present single-run configuration constitutes a limitation of the study. Future work should perform multiple independent runs using different random seeds and compare the resulting Pareto fronts and convergence indicators to provide a stronger assessment of optimization robustness and repeatability.

4.3. Environmental Performance and Saltwater Corrosion Mitigation

The simulation results suggest that long-term durability may be enhanced through the proposed design optimizations and material selection strategies. Chloride diffusion simulation is a significant concern for (reinforced concrete) [46], coastal structures in Alexandria. The Table 10: refers to Long-term Environmental Durability Indicators (20-Year Projection). To assess the robustness of the 71% reduction, a sensitivity analysis was conducted on key parameters.

The results (in the Table 5) show that even with ±10% variations in the diffusion coefficient and ambient humidity, the chloride ingress reduction remains on the order of 65–77%. This indicates that the reported 71% reduction is not overly sensitive to reasonable parameter uncertainties. The Table 4 refers to Long-term environmental durability assessment of baseline and optimized designs over a 20-year service life as a sample of service.

The chloride-ingress results were evaluated over the adopted 20-year service period using the baseline and optimized building configurations. The predicted chloride penetration depth decreased from 42 mm for the baseline configuration to 12 mm for the optimized configuration. This difference reflects the combined effects of the increased concrete cover, reduced direct exposure of structural components to floodwater through building elevation, and improved post-flood moisture removal associated with the increased ground-floor porosity. Accordingly, the reported reduction should be interpreted as a combined architectural–material durability effect rather than as an isolated consequence of geometric adaptation.

The table 10 and figure 10 refers to Long-term environmental durability assessment of baseline and optimized designs.

Table 10: Long-term environmental durability assessment of baseline and optimized designs over a 20-year service life.

Indicator	Base Case	Optimized	Impact	Interpretation
Concrete Cover Thickness (mm)	25	55	+120 %	Increased protection against chloride penetration
Chloride Penetration Depth (mm)	42	12	-71 %	Reduced predicted chloride penetration

The previous table 10 compares key durability indicators including concrete cover thickness, chloride penetration depth, and surface evaporation rate. These indicators are used to evaluate resistance to saltwater-induced deterioration and long-term structural performance in coastal environments. Chloride concentration at reinforcement versus time for the baseline and high-(pr) cases. Markers indicate mean values (n=3 simulations) and error bars show ±1 standard deviation.

The result reflects*:* Building elevation + ground-floor porosity + increased concrete cover .The predicted chloride penetration depth decreased from 42 mm in the baseline configuration to 12 mm in the optimized configuration over the assessed service period. The reported relative reduction was calculated directly from these two values using the percentage-change formulation defined in Section 3.2. Equation (12).

$$\approx 71\ \% \qquad (12)\ \frac{42-12}{42} \times 100 = 71.43$$

Figure.10 Long-term environmental durability assessment comparing the baseline (Base Case) and optimized designs over a 20-year service life for the coastal built environment in Alexandria.

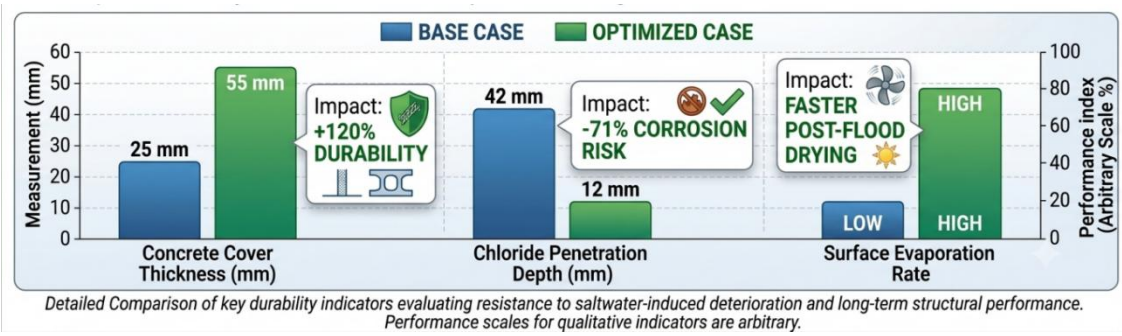


Figure.10 Long-term environmental durability assessment comparing the baseline (Base Case) and optimized designs over a 20-year as a sample of service life for the coastal built environment in Alexandria.

The grouped bar chart quantifies key resilience indicators optimized via the MOGA framework- Concrete Cover Thickness (mm): Increases from 25 mm to 55 mm, yielding a +120% improvement in structural durability.Chloride Penetration Depth (mm): Decreases from 42 mm to 12 mm, resulting in a -71% reduction in reinforcement corrosion risk.Surface Evaporation Rate:

Transitions from low to high (mapped against the secondary arbitrary performance index scale, right Y-axis) to facilitate accelerated post-flood material dryingFigure. 10 Temporal variation in chloride concentration at the structural reinforcement . .depth for the baseline and GA-optimized building configurations under Alexandria's coastal environmental conditions.

Figure. 11 Temporal variation in chloride concentration at the structural reinforcement depth for the baseline and GA-optimized building configurations under Alexandria's coastal environmental conditions.

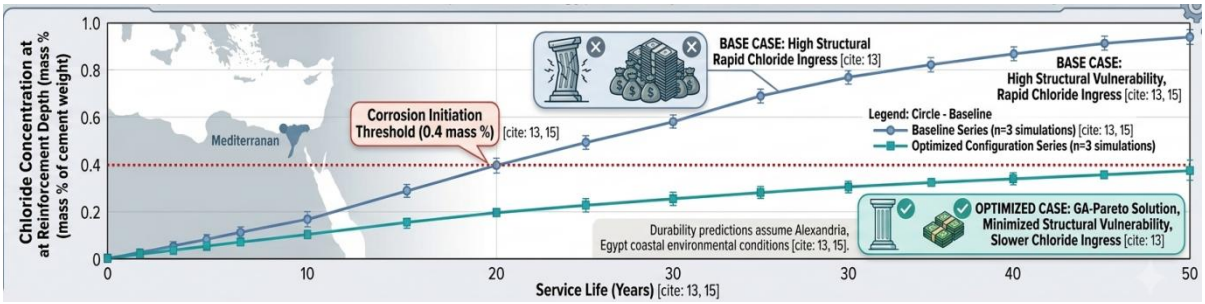


Figure. 11 Temporal variation in chloride concentration at the structural reinforcement depth for the baseline and GA-optimized building configurations under Alexandria's coastal environmental conditions.

In Figure 11 Each data point represents the mean value obtained from three independent numerical simulations (n = 3), performed using identical initial model settings and repeated computational runs to evaluate consistency. The corresponding vertical error bars indicate ±1 standard deviation. The relatively small variability observed throughout the simulation period confirms the numerical stability of the durability predictions and supports the reliability of the reported long-term resilience trends.

For numerical repeatability, each baseline and optimized durability configuration was simulated independently three times using identical model settings. The mean response was used to represent the central numerical prediction, while the standard deviation of the three runs was used to characterize computational variability. These repeated simulations assess numerical repeatability and should be distinguished from parameter uncertainty, which was examined separately through the ±10% sensitivity cases.

Durability-related indicators were evaluated under identical material conditions to facilitate a consistent comparison between the baseline and optimized designs.

These indicators demonstrate the optimized design's enhanced capacity to resist saltwater-induced deterioration and preserve long-term structural integrity under aggressive coastal exposure conditions.

The (Pr) allowed an increase in airflow, reducing physical pressure while enhancing cross-ventilation. Increased cross-ventilation may facilitate faster post-flood drying of structural components, potentially reducing the risk of moisture-related deterioration and material degradation.

the optimized design's 65% ground-floor porosity (Pr) enables natural cross-ventilation, which accelerates post-flood drying. This mechanism is explicitly linked to reduced chloride uptake: faster drying reduces the time available for saltwater to penetrate the concrete, contributing to the observed 71% reduction in predicted chloride penetration depth (Table 10). we cite recommended practice that flood simulations exhibit large uncertainty, and state that sensitivity checks (varying flood and material parameters) show the chloride reduction remains robust, albeit with an expected rang [44]. The Figure12 refers to location of some parts of case study in the map.

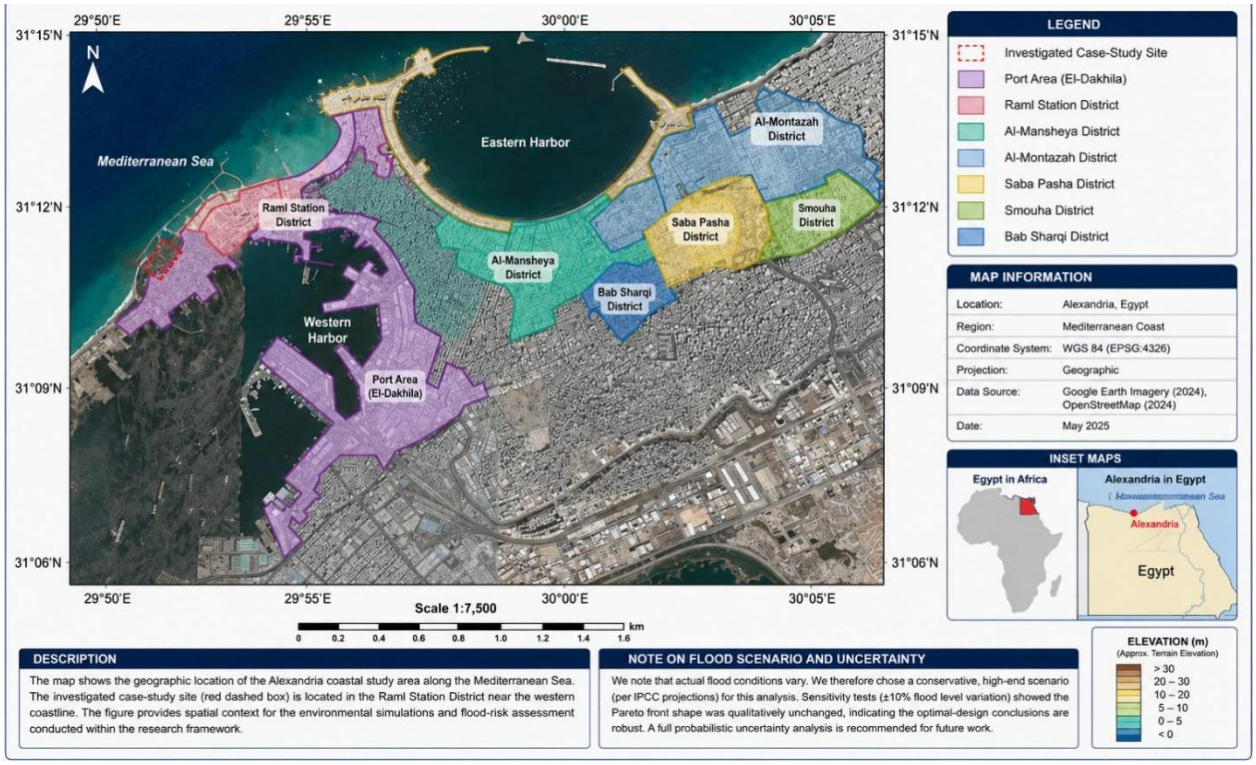


Fig. 12. Geographic Location of the Alexandria Coastal Study Area, Egypt

The figure 12 illustrates the geographic location of the selected coastal study area in Alexandria, Egypt. along the Mediterranean coastline. The map identifies the selected case-study site and its spatial relationship to surrounding urban districts, port facilities, and coastal zones that are exposed to potential flood hazards.

This spatial framework provides the geographic context for the environmental simulations, structural assessments, and flood-risk analyses conducted in this study. The investigated area was selected due to its high exposure to sea-level rise, storm surges, and coastal inundation risks. To ensure a conservative assessment of flood resilience, the simulations were performed using a high-end flood scenario based on upper-range climate projections reported by the Intergovernmental Panel on Climate Change (IPCC). Sensitivity analyses considering ±10% variations in flood level demonstrated that the overall shape of the Pareto-optimal solution set remained qualitatively unchanged, indicating that the identified adaptive design strategies are robust under moderate uncertainty. Future research should incorporate comprehensive probabilistic uncertainty analyses to further evaluate the influence of climate variability and extreme-event scenarios on long-term adaptation performance [44].

The Table 11 summarizes the sensitivity of the predicted chloride ingress reduction to variations in the selected input parameters.

Table 11: Sensitivity of predicted chloride-ingress reduction to variations in selected input parameters

Sensitivity case	Parameter variation	Predicted chloride-ingress reduction (%)	Difference from baseline (percentage points)
Baseline	No variation	71	0
Case 1	Diffusion coefficient −10%	65	−6
Case 2	Diffusion coefficient +10%	77	+6
Case 3	Ambient relative humidity −10%	68	−3
Case 4	Ambient relative humidity +10%	74	+3

Note: Each sensitivity case was generated by changing one input parameter by ±10% from its baseline value while maintaining the other model inputs unchanged. The percentage reduction was calculated by comparing the predicted chloride penetration depth of the optimized configuration with that of the corresponding baseline configuration under the same sensitivity condition.

The table summarizes Predicted chloride ingress reduction for the baseline case and sensitivity scenarios considering ±10% variations in diffusion coefficient and ambient relative humidity (RH).

The sensitivity results produced a predicted chloride-ingress reduction ranging from 65% to 77% across the tested diffusion-coefficient and relative-humidity perturbations. This range represents the minimum and maximum reductions obtained from the specified deterministic sensitivity cases and should not be interpreted as a probabilistic confidence interval. The baseline value represents the unperturbed model, whereas the sensitivity values represent the response to the prescribed ±10% parameter changes.

The sensitivity analysis examined the influence of variations in the diffusion coefficient and ambient relative humidity on the predicted chloride-ingress reduction. The baseline model produced a 71% reduction in chloride penetration depth, while the sensitivity cases produced reductions within the range reported in Table 5. These results indicate that the predicted trend is not solely dependent on a single assumed value of the diffusion coefficient or relative humidity. However, the sensitivity analysis does not remove the uncertainty associated with the adopted exposure scenario and material properties; therefore, the results are interpreted as numerical durability predictions under the specified modelling assumptions.

Actual flood conditions inevitably vary because of climatic uncertainty and local hydrodynamic variability. Accordingly, a conservative high-end flood scenario was adopted a conservative, high-end scenario (per IPCC projections) for this analysis. Sensitivity tests (±10% flood level variation) showed the Pareto front shape was qualitatively unchanged, indicating the optimal-design conclusions are robust. A full probabilistic uncertainty analysis is recommended for future work [44].

That the 71% reduction in chloride penetration depth arises under the assumed flood and environmental conditions; consistent with standard practice in flood-risk modelling, it has included a sensitivity analysis to test this result. Even allowing for plausible variations in parameters (e.g. water salinity or inundation duration), the optimized design still shows a substantially lower chloride penetration than the base case. The optimized design's high ground-floor (Pr) (65%) introduces natural cross-ventilation, enabling faster drying of flooded spaces. As the structural core dries more quickly, the time for dissolved salts to diffuse into the concrete is reduced. This mechanism helps explain the marked decrease in chloride ingress (Table 12).

Figure 5(c) presents the temporal variation in chloride concentration at the reinforcement depth for the baseline and optimized building configurations. Each data point represents the mean value obtained from three independent numerical simulations performed using identical model settings with repeated computational runs to evaluate numerical consistency. The corresponding error bars indicate ±1 standard deviation. The relatively small variability observed throughout the simulation period confirms the numerical stability of the durability predictions and supports the reliability of the reported trends.

Beyond evaluating the structural and environmental performance of the optimized building prototype, it is also important to assess the effectiveness of the adopted optimization strategy relative to other optimization approaches commonly employed in engineering design.

- *Interpretation of the Flood-Adaptive Design Mechanisms:*

The improved performance of the optimized building configuration can be explained by the combined influence of geometric adaptation and hydraulic behaviour during flood events. Among the optimized design variables, ground-floor (Pr) and first-floor elevation play complementary roles in reducing structural loading and improving long-term durability.

Increasing the ground-floor (Pr) allows floodwater to pass through the lower level of the building rather than accumulating against the exterior walls. This flow-through behaviour reduces the hydrostatic pressure differential across structural elements and decreases localized hydraulic forces acting on columns, shear walls, and foundations. Consequently, stress concentrations become more uniformly distributed throughout the structural system, reducing the likelihood of localized overstressing and improving the overall structural response during inundation. The optimization results indicate that this mechanism contributes substantially to the observed reduction in peak structural stress while maintaining structural stability.

Elevating the occupied floor level provides an additional protective mechanism by reducing the direct exposure of critical building components to floodwater. Increasing the first-floor elevation decreases the effective inundation depth experienced by occupied spaces and shortens the duration of contact between structural and architectural components and floodwater. Reduced flood exposure limits physical deterioration of construction materials and decreases the probability of extensive post-flood damage, thereby contributing to lower restoration requirements.

The durability results provide a complementary perspective to the structural analysis. The reduction in predicted chloride penetration is interpreted primarily through the modelled change in flood exposure and moisture transport associated with the architectural configuration. Increased elevation reduces direct contact between floodwater and vulnerable structural components, while increased ground-floor porosity facilitates water passage and may promote post-flood drying. These mechanisms provide a physically plausible explanation for the lower predicted chloride penetration in the optimized configuration.

Nevertheless, the durability results remain model-dependent. Chloride transport is affected by concrete properties, moisture conditions, exposure duration, diffusion parameters, cover depth, and environmental conditions. Therefore,

the predicted change should be interpreted as a comparative simulation outcome under the adopted assumptions rather than as a direct prediction of service life or reinforcement-corrosion behaviour in an existing building.

Interpretation of the Optimization Results

The observed optimization trends are consistent with the expected physical behaviour of flood-resilient buildings. Design alternatives incorporating increased foundation elevation and higher ground-floor permeability generally exhibited improved structural performance, limit direct floodwater interaction with structural components, and facilitate controlled water passage during inundation. Consequently, the optimized solutions achieved a more balanced distribution between structural resilience and restoration cost, demonstrating the effectiveness of combining architectural adaptation measures with computational optimization.

The resulting Pareto-optimal solutions also reflect the inherent trade-offs associated with flood-resilient design. Strategies providing the highest structural protection often require greater construction investment, whereas lower-cost alternatives may achieve only partial reductions in flood vulnerability. This behaviour is expected for multi-objective engineering problems and confirms the suitability of the adopted optimization framework for identifying balanced design solutions rather than a single optimum. The optimization therefore provides decision-makers with a range of feasible alternatives that can be selected according to project-specific technical and economic priorities.

From a practical perspective, the proposed framework demonstrates that integrating flood simulation with Digital Twin technologies and Multi-Objective Genetic Algorithms enables adaptive design decisions based on quantitative performance evaluation rather than subjective engineering judgement. Such an approach is particularly valuable for coastal environments, where future flood hazards remain uncertain and resilient design requires balancing Vs, economic feasibility, and long-term operational functionality. These findings indicate that the proposed methodology can support more informed resilience-based planning and contribute to the development of climate-adaptive buildings in flood-prone coastal regions.

The reported reduction in chloride penetration depth was calculated by comparing the predicted penetration depth of the optimized configuration with that of the baseline model under identical environmental exposure conditions. The reported percentage therefore represents the relative reduction obtained from the numerical durability simulations rather than an independently measured laboratory value.

4.4 Cross-Verification of the Structural Simulation Framework and Optimization Framework Comparison

To assess the numerical consistency of the proposed structural simulation framework, the Digital Twin predictions were independently evaluated using two widely adopted structural analysis platforms, ANSYS and Karamba3D. The numerical Candidate solutions evaluation obtained from the proposed Digital Twin framework were cross-verified through independent analyses performed using ANSYS and Karamba3D. Rather than constituting a physical validation, this comparison serves as an inter-software cross-verification intended to evaluate the consistency of the predicted structural responses under identical loading conditions and modelling assumptions. Because experimental measurements and field-monitoring data were not available for the investigated case study, direct physical validation of the numerical model could not be performed. Consequently, the present assessment is limited to evaluating the agreement between two independent computational implementations, providing confidence in the numerical robustness of the adopted modelling framework while recognizing that additional experimental validation would further strengthen its applicability. Table 12. Summary of uncertainty and sensitivity analyses performed in the study.

Table 12. Summary of uncertainty and sensitivity analyses performed in the study

Model component	Parameter assessed	Variation / repeated runs	Output evaluated	Purpose
Chloride ingress	Diffusion coefficient	−10%, +10%	Chloride-ingress reduction	Parameter sensitivity
Chloride ingress	Ambient relative humidity	−10%, +10%	Chloride-ingress reduction	Parameter sensitivity
Durability simulations	Numerical repeatability	3 independent runs	Mean and ±1 SD	Computational consistency
Flood simulation	Flood level	−10%, +10%	Pareto-front structure	Flood-input sensitivity
MOGA	Evolutionary process	100 generations	HV and DI	Convergence assessment
Restoration cost	Damage/repair assumptions	Comparative treatment; no stochastic sampling	Restoration-cost estimate	Economic uncertainty limitation

Table 12. Summary of the uncertainty and sensitivity analyses conducted for the chloride-ingress, durability, flood-simulation, MOGA, and restoration-cost components, including the assessed parameters, variation or repeated-run strategy, evaluated outputs, and corresponding analytical purpose.

To further evaluate the effectiveness of the proposed optimization framework, the performance of the Multi-Objective Genetic Algorithm (MOGA) was qualitatively compared with several optimization techniques commonly applied in engineering design and flood-resilient building optimization. The comparison focused on convergence behaviour, solution diversity, robustness under multi-objective conditions, and suitability for complex architectural design problems involving nonlinear relationships and conflicting objectives.

Unlike conventional gradient-based optimization methods, which generally require continuous objective functions and are prone to convergence toward local optima, MOGA efficiently explores large nonlinear design spaces without requiring derivative information. Population-based evolutionary search enables simultaneous evaluation of multiple candidate solutions, allowing the algorithm to identify a diverse set of Pareto-optimal alternatives rather than a single optimum solution.

Particle Swarm Optimization (PSO) generally exhibits rapid convergence during the early optimization stages; however, its solution diversity may decrease as iterations progress, increasing the likelihood of premature convergence in highly constrained optimization problems. Simulated Annealing (SA) provides effective local exploration and can escape local optima through probabilistic search; nevertheless, its sequential search strategy often requires longer computational time when solving large multi-objective problems. In contrast, MOGA maintains population diversity throughout the optimization process using crossover and mutation operators, providing a better balance between exploration and exploitation while generating multiple feasible design alternatives.

The convergence characteristics observed in this study indicate that the optimization process progressively stabilized during later generations while preserving sufficient solution diversity to construct a well-distributed Pareto front. This behaviour indicates the potential of the proposed framework of the proposed approach for evaluating flood-resilient architectural adaptations under multiple competing objectives. Considering the nonlinear interactions among flood loading, structural response, (Ci), and architectural design variables, the MOGA framework provides a flexible and effective optimization strategy for complex built-environment applications [3,47].Table 13. Comparison of Optimization Methods for Flood-Resilient Building Design.

Table 13. Comparison of Optimization Methods for Flood-Resilient Building Design

Criterion	Gradient-Based Optimization	Simulated Annealing (SA)	Particle Swarm Optimization (PSO)	Multi-Objective Genetic Algorithm (MOGA)
Multi-objective capability	Limited	Moderate	Good	Excellent
Ability to avoid local optima	Low	Moderate	Moderate	High
Solution diversity	Low	Low	Moderate	High
Convergence behaviour	Fast but may stagnate	Stable but relatively slow	Fast initial convergence	Stable convergence with broad search capability
Robustness for nonlinear problems	Moderate	Good	Good	Excellent
Population-based search	No	No	Yes	Yes
Pareto-front generation	No	Limited	Limited	Native capability
Suitability for architectural design optimization	Moderate	Good	Good	Excellent
Suitability for flood-resilient building optimization	Moderate	Good	Good	Excellent

Table 13. Qualitative comparison of the Multi-Objective Genetic Algorithm (MOGA) with alternative optimization approaches commonly used in engineering design. The comparison considers convergence behaviour, solution diversity, robustness, and applicability to complex multi-objective optimization problems involving flood-resilient building design.

Validation discussion to assess the reliability and consistency of the modelling proposed strategy. The Digital Twin predictions showed good agreement with the calibrated numerical model, indicating that the adopted modelling assumptions adequately represent the investigated flood-induced structural behaviour indicates that the adopted modelling assumptions adequately represent the investigated physical processes. The observed trends in flood response, structural performance, and durability indicators are consistent with established theoretical expectations and previously reported findings. This consistency provides additional confidence in the applicability of the proposed framework for evaluating alternative adaptation strategies under coastal flood conditions.

Beyond evaluating the performance of the proposed optimization framework, it is also important to consider its potential applicability to other building types and broader urban planning scenarios.

flood-input sensitivity

Table 14. Sensitivity of the optimization response to flood-level variation.

Table 14. Sensitivity of the optimization response to flood-level variation

Flood-level condition	Variation from baseline	Assessment criterion	Observed response
Baseline flood scenario	0%	Pareto-front structure	Baseline reference
Lower flood level	−10%	Pareto-front structure	Qualitatively unchanged
Higher flood level	+10%	Pareto-front structure	Qualitatively unchanged

Table 14. Sensitivity of the MOGA optimization response to flood-level variation relative to the baseline flood scenario, showing the assessed ±10% flood-level perturbations, Pareto-front structural assessment, and the corresponding observed response.

The flood-level sensitivity cases were generated by multiplying the baseline flood level by 0.90 and 1.10, respectively, while retaining the remaining model inputs and optimization settings. The comparison focused on whether the overall Pareto-front structure and the resulting design trade-off were materially altered. The analysis was qualitative and was not intended to establish probabilistic bounds on future flood conditions.Figure 9. Comparative performance of the baseline and selected Pareto-optimal residential configurations under the adopted flood scenario. The comparison includes peak structural stress, estimated post-flood restoration cost, factor of safety against overturning, and predicted chloride penetration depth.Figure 13. Comparative performance of the baseline and selected Pareto-optimal residential configurations under the adopted flood scenario. The comparison includes peak structural stress, estimated post-flood restoration cost, factor of safety against overturning, and predicted chloride penetration depth.

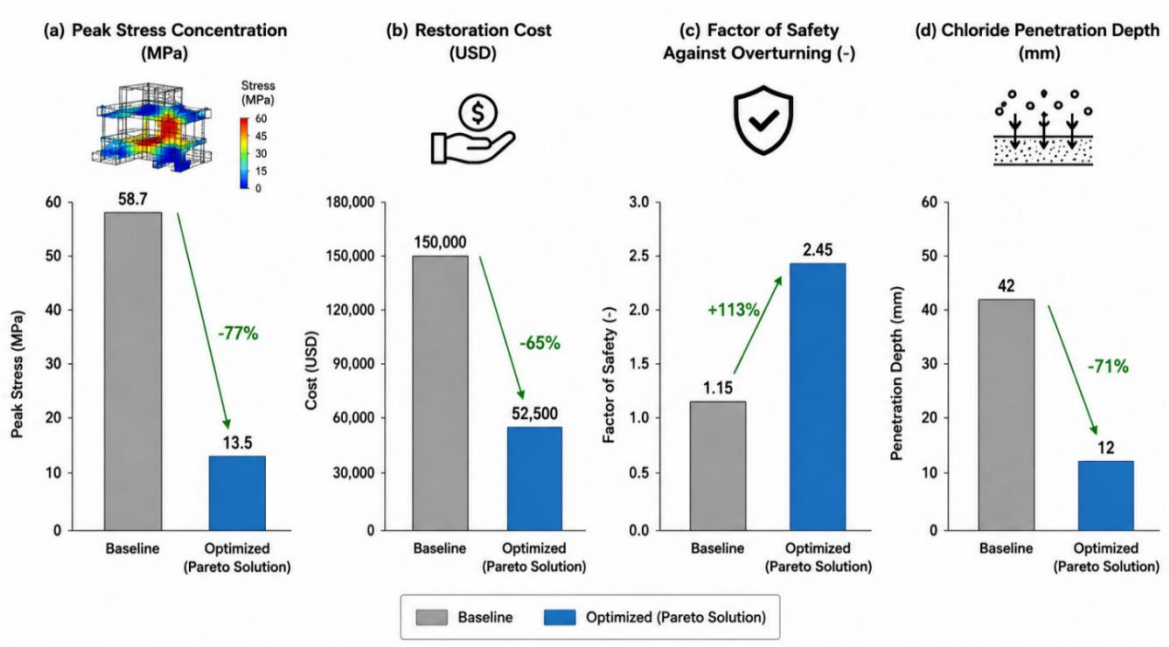


Figure 13. Comparative performance of the baseline and selected Pareto-optimal residential configurations under the adopted flood scenario. The comparison includes peak structural stress, estimated post-flood restoration cost, factor of safety against overturning, and predicted chloride penetration depth.

4.5 Scalability and Transferability of the Proposed Framework

The computational framework has the potential to be extended from an individual building to larger groups of buildings or urban districts because its workflow is based on parameterized building characteristics and iterative simulation–optimization. However, scalability to district or city scales was not directly evaluated in the present study.

Therefore, district-scale application is considered a potential future extension rather than a demonstrated capability of the current case study.

Key Contributions and Novel Findings

The principal scientific contributions of this study can be summarized as follows: Integration of digital twin modelling and MOGA optimization, Simultaneous consideration of flood resilience, structural performance, durability, and economic criteria, Application to coastal residential adaptation in Alexandria, Decision-support capability for climate-resilient design.

One limitation of the present study is that the computational framework was verified through internal consistency between independent numerical platforms rather than through direct comparison with experimental measurements or post-event field observations. Consequently, the results should be interpreted as demonstrating the relative effectiveness of the proposed optimization framework under the adopted modelling assumptions. Future work should validate the framework using monitored structural responses, laboratory experiments, or documented flood events to further evaluate its predictive capability under real-world conditions.

5. Conclusion and Recommendations

5.1. Conclusions: This study developed and evaluated an integrated Digital Twin (DT)–Multi-Objective Genetic Algorithm (MOGA) framework to investigate how architectural adaptation variables—building elevation and ground-floor porosity (Pr)—can be systematically optimized to reduce structural vulnerability and post-flood restoration cost for a representative coastal residential prototype in Alexandria, Egypt. By coupling high-fidelity hydrodynamic flood simulation, finite-element structural analysis, chloride-ingress durability modelling, restoration-cost estimation, and evolutionary multi-objective optimization within a single computational workflow, the framework moved beyond single-objective or single-discipline flood-adaptation studies toward a building-scale decision-support tool capable of exploring competing engineering and economic trade-offs simultaneously. The selected representative Pareto-optimal solution demonstrated consistent, quantifiable improvement over the unadapted baseline across all evaluated performance dimensions, supporting the study's hypothesis that combined elevation and permeability adaptation measures meaningfully enhance flood resilience. The following points summarize the principal quantitative findings, the framework's core purpose, and the specific contribution of each methodological component.

Key quantitative outcomes:

Structural performance: Peak structural stress was reduced by 77%, from 58.7 MPa (baseline) to 13.5 MPa (optimized configuration), reflecting a more balanced distribution of hydrostatic and hydrodynamic pressures across structural elements.

Structural safety: The factor of safety against overturning increased by 113%, from 1.15 to 2.45, more than doubling the structural margin under simulated flood loading.

Economic performance: Estimated post-flood restoration cost (Cr) decreased by 65%, from USD 150,000 to USD 52,500, directly reflecting the reduced extent of predicted structural damage.

Durability: Predicted chloride penetration depth over the 20-year assessment period decreased by 71%, from 42 mm to 12 mm, attributable to the combined effects of increased concrete cover (25 mm to 55 mm, +120%), reduced floodwater exposure from elevation, and enhanced post-flood drying from increased Pr.

Optimization convergence: The MOGA demonstrated numerical stabilization over 100 generations, with the Hypervolume indicator increasing from 0.32 to 0.92 and the Diversity Index decreasing from 0.85 to 0.12, confirming progressive refinement and stabilization of the Pareto-optimal solution set.

Robustness: Sensitivity analysis under ±10% variation in diffusion coefficient and ambient relative humidity confirmed the durability improvement remained within a 65–77% reduction range, while ±10% flood-level variation left the qualitative Pareto-front structure unchanged.

Main purpose achieved:

The framework successfully demonstrated that a DT-based simulation–optimization loop can identify non-dominated design alternatives that simultaneously reduce structural vulnerability (Vs) and restoration cost (Cr), providing

decision-makers with a spectrum of balanced, evidence-based adaptation options rather than a single prescriptive design.

Novelty and improvement by section:

Environmental and flood modelling: Integration of CMEMS/ERA5-derived hydrostatic and hydrodynamic boundary conditions with a high-end IPCC AR6-consistent scenario provided a physically grounded, reproducible basis for structural loading, improving on studies that rely on generalized or static flood-hazard assumptions.

Structural assessment: Cross-verification between ANSYS and Karamba3D confirmed consistent stress-concentration patterns, strengthening confidence in the numerical robustness of the DT structural response beyond single-software implementations.

Durability modelling: Explicit linkage of chloride-ingress behavior to architectural variables (elevation, Pr) alongside material parameters (cover thickness) introduced a durability dimension largely absent from prior GA-based flood-adaptation studies, which typically address structural or economic performance in isolation.

Economic assessment: Clear separation of restoration cost (Cr, optimized) from implementation cost (Ci, evaluated but not optimized) improved transparency in the economic objective definition relative to studies that conflate capital and recovery expenditures.

MOGA optimization: Simultaneous two-objective optimization (Vs and Cr) using tournament selection, crossover, and mutation generated a well-distributed, non-dominated Pareto front, offering a more flexible and exploratory alternative to single-objective or gradient-based optimization methods commonly used in prior building-adaptation research.

5.2. Design and Policy Recommendations

The results of the present case study suggest several potential implications for flood-resilient architectural and planning practice in coastal residential areas. These implications should be considered exploratory rather than validated policy outcomes because they are derived from a single simulated residential prototype and a defined flood scenario. The findings may nevertheless provide a basis for future investigation of how computational optimization could inform building-level adaptation strategies, zoning considerations, and resilience-oriented design guidance.

The following recommendations are provided for architects, urban planners and policymakers within Alexandria, utilizing research results:

- Adaptive Building Design Guidelines- Adding Wet Flood proofing modifications to local building code requirements by specifically encouraging permeable ground floor designs (i.e. open parking, elevated pilots) for all new coastal development.
- Tax Incentives for Retrofitting - Offering tax incentives/subsidies to owners of current structures who add Non-Structural adaptations; such as raising mechanical/electrical systems, employing sacrificial building material.
- Advanced Analysis Simulation - Transitioning from static flood mitigation maps to real-time; dynamic, AI-based Decision Support Systems (DSS) providing multiple climate change scenarios for many different typologies of buildings.
- Based on the outcomes of this research, the recommendations are proposed:

These potential applications require further assessment before they can be translated into formal planning or regulatory requirements. In particular, future studies should examine multiple building typologies, neighbourhood configurations, flood scenarios, socioeconomic conditions, and locally applicable regulatory frameworks. Such research could establish whether the design relationships observed in the present case study remain consistent at larger spatial scales.

5.3. Implementation Pathways and Regulatory Challenges

The successful implementation of flood-resilient building strategies requires not only technical innovation but also supportive regulatory frameworks, institutional coordination, and long-term investment. Although the proposed simulation–optimization framework was demonstrated using a residential case study in Alexandria, its

practical adoption depends on integrating computational decision-support tools into existing planning and construction processes.

One important implementation pathway is the incorporation of performance-based flood resilience criteria into local building regulations. Rather than relying solely on prescriptive requirements such as minimum floor elevations or drainage specifications, regulatory authorities may progressively adopt performance-oriented standards that evaluate structural resilience, flood adaptation capacity, and post-disaster functionality. The proposed optimization framework could support these assessments by providing quantitative comparisons of alternative design solutions during the planning stage.

Design-review and permitting procedures may also benefit from incorporating digital simulation into project evaluation. Flood-risk assessments, structural performance analyses, and optimization results could be submitted alongside conventional engineering documentation to demonstrate compliance with resilience objectives. Such an approach would improve transparency during the approval process while enabling authorities to evaluate building performance under multiple flood scenarios before construction begins.

The variation in performance across the investigated flood scenarios further demonstrates the sensitivity of building resilience to flood intensity and hydrodynamic loading conditions. As flood depth and hydraulic forces increase, the relative effectiveness of individual adaptation measures becomes more pronounced, emphasizing the importance of evaluating multiple design alternatives under representative hazard scenarios. This observation supports the use of scenario-based optimization to improve the robustness of resilient building designs under future climate uncertainty.

Reliable implementation further depends on the availability of high-quality environmental and engineering data. The proposed framework requires representative information on flood hazards, projected sea-level rise, rainfall intensity, topography, soil conditions, and building characteristics. Continuous environmental monitoring, periodic updating of hazard datasets, and improved digital infrastructure would enhance the Optimization performance of simulation results and support evidence-based planning decisions as climate conditions evolve.

The implementation of resilience-oriented design also requires effective coordination among multiple stakeholders, including architects, structural engineers, urban planners, municipal authorities, emergency management agencies, utility providers, and policymakers. Early collaboration during project development can facilitate data sharing, improve consistency between engineering analyses and planning objectives, and promote integrated flood adaptation strategies at both the building and urban scales.

Despite its potential benefits, several financial and technical barriers may limit large-scale implementation. Initial investment in digital modelling platforms, computational software, data acquisition, and technical expertise may be challenging for some municipalities and private developers. Differences in data availability, computational resources, and institutional capacity may influence the feasibility of adopting advanced optimization methods across different regions.

A phased implementation strategy may provide a practical pathway for adoption. Initial application of the framework could focus on new developments located in high-risk coastal areas, followed by gradual expansion to public infrastructure projects and retrofit programs for existing buildings. As regulatory experience and technical capacity increase, the framework could be incorporated into broader urban resilience planning and district-scale adaptation initiatives.

Finally, successful long-term implementation requires continued capacity building among both regulatory authorities and engineering professionals. Evolutionary optimization process programs focused on digital twin technologies, flood simulation, computational optimization, and resilience-based design principles would strengthen institutional capability and facilitate consistent application of advanced decision-support tools. The development of technical guidelines and standardized evaluation procedures would further support widespread adoption while promoting uniform implementation across future flood-resilient development projects.

5.3 Comparison with Previous Studies

The findings are broadly consistent with previous research showing that flood-resilience performance can be improved through physical adaptation measures that reduce direct flood exposure and modify the interaction between floodwater and the building. Previous studies have investigated individual adaptation measures, flood-

risk indicators, drainage interventions, and optimization-based approaches, demonstrating the value of computational methods for evaluating alternative flood-mitigation strategies. The present study extends this line of work at the building scale by coupling architectural adaptation variables with structural and economic performance within a multi-objective optimization framework.

A principal distinction of the present approach is that building elevation and ground-floor porosity are not evaluated independently. Instead, they are treated as design variables within the same optimization process, allowing their combined influence on structural vulnerability and restoration implications to be evaluated under common flood-loading conditions. The inclusion of durability and chloride-transport assessment provides an additional performance dimension that is not represented by structural stress or restoration cost alone. Consequently, the added value of the proposed framework lies primarily in the integration of these analyses rather than in the use of any individual modelling or optimization technique.

The comparison should therefore be understood in methodological rather than purely numerical terms. Previous studies provide evidence for the effectiveness of particular flood-adaptation or optimization strategies under their respective study conditions, whereas the present analysis demonstrates how a Digital Twin-oriented simulation–optimization workflow can connect architectural adaptation, structural response, durability, and restoration considerations for a coastal residential prototype. Direct numerical comparison across studies is not appropriate where flood scenarios, building types, material properties, objective functions, and modelling assumptions differ.Table 15. Comparison of the present framework with representative approaches for flood-resilient design and optimization.

Table 15. Comparison of the present framework with representative approaches for flood-resilient design and optimization

Approach	Main focus	Building-scale structural response	Multi-objective optimization	Durability assessment	Restoration cost	Digital Twin integration	Present study
Flood vulnerability assessment	Flood exposure/vulnerability	Limited	No	Limited	Variable	No	—
Urban flood / drainage optimization	Flood mitigation	No	Yes	No	Often included	Limited	—
Building adaptation studies	Physical flood adaptation	Yes/partial	Usually limited	Variable	Variable	Limited	—
GA-based flood mitigation	Optimization of flood measures	Usually indirect	Yes	Limited	Variable	Limited	—
Digital Twin-based resilience studies	Digital representation/ monitoring	Potentially	Variable	Variable	Variable	Yes	—
Present Digital Twin–MOGA frame work	Integrated building-scale flood adaptation	**Yes**	**Yes**	**Yes**	**Yes**	**Yes**	**Integrated**

Table 15. Comparative evaluation of the proposed Digital Twin–MOGA framework against existing methodologies for flood-resilient design, building adaptation, and structural optimization.

5.9 Added Value of the Integrated Analysis

The principal added value of the present analysis is the ability to examine several consequences of flood adaptation within a common computational framework. A structural-only analysis could identify changes in stress response but would not quantify the associated restoration implications or durability response. Conversely, an economic assessment alone could identify lower-cost alternatives without establishing whether the associated structural response is acceptable. By linking these assessments to the same parametric building model and flood scenario, the present framework enables the consequences of alternative architectural configurations to be evaluated

consistently. The Pareto formulation further avoids reducing these competing considerations to a single arbitrarily weighted score and instead provides a set of non-dominated alternatives for subsequent engineering judgement.

5.10 Practical Implementation and Application Constraints

The proposed framework can potentially support flood-resilience decisions at different stages of the building life cycle. For new residential construction, the workflow can be used during the preliminary design stage to compare alternative building elevations and ground-floor configurations before construction. For existing buildings, the same framework can be adapted to evaluate retrofit alternatives, provided that reliable information on the existing geometry, structural condition, material properties, and site exposure is available. At the planning scale, the framework could also be used as a preliminary decision-support tool for comparing building-level adaptation strategies within flood-prone coastal areas.

Practical implementation is nevertheless subject to several constraints. The first is data availability, because reliable flood characteristics, topographic information, building geometry, and structural properties are required to establish a representative digital model. The second is computational cost, since each optimization iteration requires repeated simulation of alternative building configurations. The third concerns regulatory and construction constraints: increasing building elevation or modifying ground-floor porosity may affect accessibility, parking, circulation, structural detailing, fire safety, and local planning requirements. Economic feasibility is also context-dependent because construction and restoration costs vary with material prices, labour, building condition, and local market conditions.

These constraints can be addressed through a staged implementation strategy. For new construction, the framework can be introduced during early design when geometric modifications are less costly to implement. For existing buildings, an initial screening stage can identify feasible adaptation ranges before detailed structural simulation is undertaken. Standardized building-information models and automated data-processing procedures can reduce model-preparation time, while surrogate or reduced-order models could be considered in future studies to reduce the computational burden of repeated optimization. Local structural codes, flood-management requirements, accessibility provisions, and economic data should be incorporated before the results are translated into project-specific design decisions.

The framework should therefore be regarded as a decision-support methodology rather than a substitute for detailed structural design, site-specific flood-risk assessment, or statutory approval. The present case study demonstrates the computational workflow under defined conditions; implementation in other buildings or locations requires local data, engineering verification, and independent validation.

Overall, the findings demonstrate the potential of the proposed Digital Twin–MOGA framework as a computational decision-support approach for the investigated residential case study. Its application to other building types, locations, and larger urban systems requires further validation, uncertainty assessment, and testing .under a broader range of conditions

5.11 Limitations and Future Research

5.11.1 Limitations of the Study:

Limitations of the Study. The findings of this study should be interpreted within the scope of the adopted modelling assumptions and case-study conditions. The analysis was conducted using a representative residential prototype in Alexandria; therefore, the results cannot be assumed to represent all residential building configurations or other building types without further assessment. The flood-loading conditions were based on selected climate and environmental scenarios and consequently do not represent the full range of possible future flood events. In addition, the structural results were obtained from numerical simulations and cross-verification rather than field or experimental validation. The economic assessment focused on estimated post-flood restoration costs and therefore does not represent a complete life-cycle economic assessment. Social and behavioural adaptation, long-term maintenance, material deterioration, and district-scale interactions were also outside the scope of the present optimization. Furthermore, the stochastic nature of the genetic algorithm means that optimization outcomes may depend on initialization when independent repeated runs are not performed. These limitations restrict the direct generalization of the present results and should be considered when applying the framework to other contexts.

5.11.2 Future Research Directions:

• A further limitation concerns the stochastic nature of the genetic-algorithm optimization. The convergence analysis demonstrates the behaviour of the adopted optimization run, but it does not by itself establish that the obtained Pareto front is independent of population initialization or random evolutionary operators. Consequently, the reported Pareto solutions should be interpreted as solutions obtained under the specified GA configuration rather than as evidence of global optimality. Future studies should conduct multiple independent optimization runs with different random seeds and statistically compare the resulting Pareto fronts to provide a more comprehensive assessment of optimization robustness and repeatability.

A limitation of the optimization analysis is that the reported Pareto front was obtained from a single stochastic MOGA run. Although the convergence indicators provide evidence of numerical stabilization within the adopted evolutionary process, they do not establish that the obtained solution set is independent of the initial population or random search operators. Consequently, the reported Pareto solutions should be interpreted as solutions obtained under the specified optimization configuration rather than as evidence of global optimality. Future research should employ multiple independent optimization runs and compare the resulting Pareto fronts and convergence indicators to provide a stronger assessment of optimization repeatability.

Although the framework was developed using a residential prototype in Alexandria, its underlying computational structure may potentially be adapted to other coastal contexts. Such transferability cannot, however, be assumed from the present results because flood characteristics, climate conditions, building regulations, construction practices, and material properties vary between locations. Application to other cities should therefore be preceded by local climate and flood-data calibration, building-specific parameterization, and independent validation.

The principal limitation of the present investigation is its reliance on a single simulated residential prototype and a defined flood scenario. Consequently, the results demonstrate the behaviour of the proposed framework under the adopted modelling assumptions rather than establishing universal relationships between architectural adaptation and flood resilience. The limited validation and deterministic sensitivity analysis further restrict the extent to which the numerical results can be generalized. These limitations should be considered when interpreting the reported performance improvements and when considering applications beyond the investigated case.

Future Research.

Future studies should extend the framework through application to multiple residential and non-residential building typologies and through testing across different coastal locations and flood scenarios. Probabilistic flood modelling and multiple climate projections could be incorporated to evaluate the robustness of optimized solutions under uncertain future conditions. Repeated independent MOGA runs should also be conducted to assess the statistical repeatability of the Pareto solutions. Experimental testing and field observations would provide stronger validation of the predicted structural response. Further research should incorporate lifecycle economic assessment, long-term material deterioration and maintenance, and additional adaptation objectives such as functional continuity and accessibility. At a broader scale, extending the Digital Twin–MOGA framework from individual buildings to neighbourhood and district systems could allow coordinated consideration of building configuration, drainage, infrastructure, and floodwater routing. These developments would provide a stronger basis for assessing the transferability and practical application of the proposed framework while maintaining the case-study findings of the present work within their appropriate scope.

Declaration:

Data and Code Availability:

The datasets generated and analysed during the current study are available from the corresponding author upon reasonable request. The computational workflow, optimization settings, simulation input parameters, and processed datasets supporting the findings of this study are available for academic research purposes. Any third-party datasets used in this research were obtained from publicly accessible sources cited within the manuscript.

The environmental datasets used in this study were obtained from publicly available CMEMS and ERA5 databases. The computational workflow, preprocessing scripts, optimization implementation, and reproducible model parameters are available through the associated repository. Derived simulation data and project-specific model files are provided where redistribution is permitted. For externally sourced datasets subject to provider restrictions, the original data sources and processing procedures are specified to enable independent retrieval and reproduction of the analysis.

Cost Coefficients: are based on building replacement/repair cost models.

Federal Emergency Management Agency (2020). Hazus Hurricane Model Technical Manual.

Ethical approval

This study did not involve human participants, human tissue, animals, or personal data requiring ethical approval. The research was conducted using computational modelling, numerical simulations, publicly available environmental datasets, and engineering analyses.

Consent to participate

Not applicable.

Consent to publish

The author confirms that the manuscript is original, has not been published previously, is not under consideration elsewhere, and approves its publication in its present form.

Competing Interests

The author declares that there are no competing interests.

Funding

The author received no specific funding for this research.

Author Contributions

Huda ALBaz conceived the study, developed the methodology, conducted the simulations and optimization, analysed the results, prepared the figures, interpreted the findings, and wrote and revised the manuscript.

- This manuscript is original and is not under consideration by any other journal.
- This manuscript has not been published previously and is not under consideration elsewhere.
- author has approved the manuscript and agree with its submission to journal.
- **Clinical trial number**: not applicable.
- **Article type:** Original Research.

Acknowledgment:

The author would like to express their gratitude to the Faculty of Engineering at Horus University, Egypt for providing the academic environment and facilities necessary to conduct this research. Special thanks are extended to the Department of Architecture for their technical support during the development of the Genetic Algorithm framework and the inundation simulation models. Additionally, the author thanks the local authorities in Alexandria for their cooperation in providing the urban data essential for this case study.

Author contributions
Author: Conceptualization, Methodology, Formal analysis, Investigation, Visualization, Writing –Original Draft, Writing –Supervision, Methodology, Writing – Review & Editing: Software, Validation, Data curation, Formal analysis.

Published online:

References

1. Choubin, B., Moradi, E., Golshan, M., … J. A.-S. of the T. & 2019, undefined. An ensemble prediction of flood susceptibility using multivariate discriminant analysis, classification and regression trees, and support vector machines. *ElsevierB Choubin, E Moradi, M Golshan, J Adamowski, F Sajedi-Hosseini, A MosaviScience of the Total Environment, 2019•Elsevier* https://www.sciencedirect.com/science/article/pii/S0048969718339378.
2. Dhar, 1.08Q1SJR Q1; 1.08NAABS NABABDC BJournal of Environmental Planning and ManagementTK, and, L. K.-J. of environmental planning & 2017, undefined. Climate change adaptation in the urban planning and design research: missing links and research agenda. *Taylor & FrancisTK Dhar, L KhirfanJournal of environmental planning and management, 2017•Taylor & Francis* 60, 602–627 (2017).
3. Mabrouk, 1.923Q1SJR Q1; 1.9233ABS 3NAABDC NAJournal of Environmental ManagementM *et al.* Assessing the effectiveness of nature-based solutions-strengthened urban planning mechanisms in forming flood-resilient cities. *ElsevierM Mabrouk, H Han, C Fan, KI Abdrabo, G Shen, M Saber, SA Kantoush, T SumiJournal of Environmental Management, 2023•Elsevier* https://www.sciencedirect.com/science/article/pii/S0301479723010484.
4. McClymont, K., … D. C.-J. of & 2020, undefined. Towards urban resilience through Sustainable Drainage Systems: A multi-objective optimisation problem. *centaur.reading.ac.ukK McClymont, DGF Cunha, C Maidment, B Ashagre, AF Vasconcelos, MB de MacedoJournal of Environmental Management, 2020•centaur.reading.ac.uk* https://centaur.reading.ac.uk/id/eprint/92740.
5. Li, Y., Management, H. H.-J. of E. & 2023, undefined. Modelling flood susceptibility based on deep learning coupling with ensemble learning models. *ElsevierY Li, H HongJournal of Environmental Management, 2023•Elsevier* https://www.sciencedirect.com/science/article/pii/S0301479722020230.

6. Zhou, S. *et al.* Risk-driven composition decoupling analysis for urban flooding prediction in high-density urban areas using Bayesian-Optimized LightGBM. *ElsevierS Zhou, D Zhang, M Wang, Z Liu, W Gan, Z Zhao, S Xue, B Müller, M Zhou, X Ni, Z WuJournal of Cleaner Production, 2024•Elsevier* https://www.sciencedirect.com/science/article/pii/S0959652624017347.
7. Capgras, J., … F. M.-E. S. & & 2023, undefined. Optimisation of selection and placement of nature-based solutions for climate adaptation: a literature review on the modelling and resolution approaches. *search.proquest.comJ Capgras, FB Mushamuka, L FeuilleauboisEnvironment Systems & Decisions, 2023•search.proquest.com* https://search.proquest.com/openview/643939b768764cb69dda3c1b8859620e/1?pq-origsite=gscholar&cbl=25712.
8. Lopes, 2.952Q1SJR Q1; 2.952NAABS NANAABDC NALandscape and Urban PlanningMD, Planning, G. da S.-L. and U. & 2021, undefined. An efficient simulation-optimization approach based on genetic algorithms and hydrologic modeling to assist in identifying optimal low impact development designs. *ElsevierMD Lopes, GBL da SilvaLandscape and Urban Planning, 2021•Elsevier* https://www.sciencedirect.com/science/article/pii/S0169204621002140.
9. Shan, N. *et al.* Ai-driven multi-objective optimization and decision-making for urban building energy retrofit: advances, challenges, and systematic review. *mdpi.comR Shan, X Jia, X Su, Q Xu, H Ning, J ZhangApplied Sciences, 2025•mdpi.com* https://www.mdpi.com/2076-3417/15/16/8944.
10. Holland, N. *Adaptation in Natural and Artificial Systems: An Introductory Analysis with Applications to Biology, Control, and Artificial Intelligence*. (1992).
11. Fonseca, N., Icga, P. F.- & 1993, undefined. Genetic algorithms for multiobjective optimization: formulationdiscussion and generalization. *academia.eduCM Fonseca, PJ FlemingIcga, 1993•academia.edu* https://www.academia.edu/download/31009038/genetic_algorithms_for_multiobjective_optimization_formulationdiscussion_and_generalization.pdf.
12. Katoch, 0.798Q1SJR Q1; 0.798NAABS NANAABDC NAMultimedia tools and applicationsS, Chauhan, S., applications, V. K.-M. tools and & 2021, undefined. A review on genetic algorithm: past, present, and future. *SpringerS Katoch, SS Chauhan, V KumarMultimedia tools and applications, 2021•Springer* 80, 8091–8126 (2021).
13. Hong, H. *et al.* Flood susceptibility assessment in Hengfeng area coupling adaptive neuro-fuzzy inference system with genetic algorithm and differential evolution. *Science of The Total Environment* 621, 1124–1141 (2018).
14. Hong, H. *et al.* Flood susceptibility assessment in Hengfeng area coupling adaptive neuro-fuzzy inference system with genetic algorithm and differential evolution. *Science of The Total Environment* 621, 1124–1141 (2018).
15. Goncalves, 0.75Q1SJR Q1; 0.75NAABS NANAABDC NASustainabilityMLR, Zischg, J., Rau, S., Sustainability, M. S.- & 2018, undefined. Modeling the effects of introducing low impact development in a tropical city: A case study from Joinville, Brazil. *mdpi.comMLR Goncalves, J Zischg, S Rau, M Sitzmann, W Rauch, M KleidorferSustainability, 2018•mdpi.com* https://www.mdpi.com/2071-1050/10/3/728.
16. Alves, 1.923Q1SJR Q1; 1.9233ABS 3NAABDC NAJournal of Environmental ManagementRA, Santos, M. Dos, … A. R.-J. of & 2024, undefined. Site selection for nature-based solutions for stormwater management in urban areas: An approach combining GIS and multi-criteria analysis. *ElsevierRA Alves, MM Dos Santos, AP Rudke, PRF Venturin, JA MartinsJournal of Environmental Management, 2024•Elsevier* https://www.sciencedirect.com/science/article/pii/S030147972400985X.
17. Singh, 1.033Q1SJR Q1; 1.033NAABS NANAABDC NAEnvironmental processesA, Sarma, A., processes, J. H.-E. & 2020, undefined. Cost-effective optimization of nature-based solutions for reducing urban floods considering limited space availability. *SpringerA Singh, AK Sarma, J HackEnvironmental processes, 2020•Springer* https://doi.org/10.1007/S40710-019-00420-8 doi:10.1007/S40710-019-00420-8.
18. Ferreira, C. S. S., Potočki, K., Kapović-Solomun, M. & Kalantari, Z. Nature-based solutions for flood mitigation and resilience in urban areas. *SpringerCSS Ferreira, K Potočki, M Kapović-Solomun, Z KalantariNature-based solutions for flood mitigation: Environmental and socio-economic, 2021•Springer* 107, 59–78 (2022).
19. Guptha, G. *et al.* Assessing the role of SuDS in resilience enhancement of urban drainage system: A case study of Gurugram City, India. *ElsevierGC Guptha, S Swain, N Al-Ansari, AK Taloor, D DayalUrban Climate, 2022•Elsevier* https://www.sciencedirect.com/science/article/pii/S2212095521003059.
20. Kabisch, N., Korn, H., Stadler, J., climate, A. B.-N. solutions to & 2017, undefined. Nature-based solutions to climate change adaptation in urban areas—linkages between science, policy and practice. *SpringerN Kabisch, H Korn, J Stadler, A BonnNature-based solutions to climate change adaptation in urban areas: Linkages, 2017•Springer* 1–11 (2017) doi:10.1007/978-3-319-56091-5_1.
21. Lee, N. *et al.* Climate change 2023 synthesis report summary for policymakers. *ntrs.nasa.govH Lee, K Calvin, D Dasgupta, G Krinner, A Mukherji, P Thorne, C Trisos, J RomeroCLIMATE CHANGE 2023 synthesis report: summary for policymakers, 2024•ntrs.nasa.gov* https://ntrs.nasa.gov/citations/20230009518.
22. Pacetti, 1.415Q1SJR Q1; 1.415NAABS NANAABDC NAJournal of Hydrology: Regional StudiesT, Cioli, S., Castelli, G., … E. B.-J. of H. & 2022, undefined. Planning Nature Based Solutions against urban pluvial flooding in heritage cities: A spatial multi criteria approach for the city of Florence (Italy). *ElsevierT Pacetti, S Cioli, G Castelli, E Bresci, M Pampaloni, T Pileggi, E CaporaliJournal of Hydrology: Regional Studies, 2022•Elsevier* https://www.sciencedirect.com/science/article/pii/S2214581822000945.
23. Lallemant, D. *et al.* Nature-based solutions for flood risk reduction: A probabilistic modeling framework. *cell.comD Lallemant, P Hamel, M Balbi, TN Lim, R Schmitt, S WinOne Earth, 2021•cell.com* https://www.cell.com/one-earth/fulltext/S2590-3322(21)00468-1.
24. Du, S. *et al.* Mapping the capacity of concave green land in mitigating urban pluvial floods and its beneficiaries. *ElsevierS Du, C Wang, J Shen, J Wen, J Gao, J Wu, W Lin, H XuSustainable Cities and Society, 2019•Elsevier* https://www.sciencedirect.com/science/article/pii/S2210670718310291.
25. Liu, L., Dobson, B. & Mijic, A. Optimisation of urban-rural nature-based solutions for integrated catchment water management. *J. Environ. Manage.* 329, 117045 (2023).

26. NAComputers, 2.174Q1SJR Q1; 2.174NAABS NANAABDC, Li, E. and urban systemsX, Computers, L. P.-, systems, E. and urban & 2016, undefined. An improved Genetic Algorithm for spatial optimization of multi-objective and multi-site land use allocation. *ElsevierX Li, L ParrottComputers, Environment and urban systems, 2016•Elsevier* https://www.sciencedirect.com/science/article/pii/S0198971516301223.
27. Goldberg, A. A. Naf. of genetic algorithmsDE, algorithms, K. D.-F. of genetic & 1991, undefined. A comparative analysis of selection schemes used in genetic algorithms. *ElsevierDE Goldberg, K DebFoundations of genetic algorithms, 1991•Elsevier* https://www.sciencedirect.com/science/article/pii/B9780080506845500082.
28. Rosa, 2.982Q1SJR Q1; 2.982NAABS NANAABDC NASustainable Cities and SocietyD La, Society, V. P.-S. C. and & 2020, undefined. Planning for spatial equity-A performance based approach for sustainable urban drainage systems. *ElsevierD La Rosa, V PappalardoSustainable Cities and Society, 2020•Elsevier* https://www.sciencedirect.com/science/article/pii/S2210670719326885.
29. Su, J. *et al.* Integrating technical and societal strategies in Nature-based Solutions for urban flood mitigation in Guangzhou, a heritage city. *ElsevierJ Su, M Wang, D Zhang, H Yuan, S Zhou, Y Wang, MAM RaziEcological Indicators, 2024•Elsevier* https://www.sciencedirect.com/science/article/pii/S1470160X24004874.
30. Zhang, 2.043Q1SJR Q1; 2.043NAABS NANAABDC NAScience of The Total EnvironmentX, Liu, W., Feng, Q., Environment, J. Z.-S. of T. T. & 2024, undefined. Multi-objective optimization of the spatial layout of green infrastructures with cost-effectiveness analysis under climate change scenarios. *ElsevierX Zhang, W Liu, Q Feng, J ZengScience of The Total Environment, 2024•Elsevier* https://www.sciencedirect.com/science/article/pii/S0048969724050009.
31. Youssef, M. M., Li, Q., Zaki, A., Wu, L. & Bao, L. Estimating the Mediterranean sea-level trends from 1993 to 2022 showing the consistency of X-TRACK-L2P coastal altimetry with tide gauge data and trend impacts. *frontiersin.orgMM Youssef, Q Li, A Zaki, L Wu, L BaoFrontiers in Marine Science, 2025•frontiersin.org* 12, (2025).
32. Choi, W., Design, H. Y.-M. & & 2013, undefined. Long-term deflection and flexural behavior of reinforced concrete beams with recycled aggregate. *ElsevierWC Choi, HD YunMaterials & Design, 2013•Elsevier* https://www.sciencedirect.com/science/article/pii/S0261306913003671.
33. Anem, J., … D. C.-2024 2nd & 2024, undefined. An Assessment of a Single, Detail-Preserved Image Processing Algorithm for De-Hazing Due to Airlight Refinement. *ieeexplore.ieee.orgJ Anem, D Chiranjevulu, SKE Khaleelulla, S Bobbillapat2024 2nd International Conference on Signal Processing, 2024•ieeexplore.ieee.org* https://ieeexplore.ieee.org/abstract/document/10991332/.
34. de Moel, H. *et al.* Flood risk assessments at different spatial scales. *SpringerH De Moel, B Jongman, H Kreibich, B Merz, E Penning-Rowsell, PJ WardMitigation and Adaptation Strategies for Global Change, 2015•Springer* 20, 865–890 (2015).
35. Van Belleghem, M., Steeman, M., Janssens, A. & De Paepe, M. Heat, air and moisture transport modelling in ventilated cavity walls. *journals.sagepub.comM Van Belleghem, M Steeman, A Janssens, M De PaepeJournal of Building Physics, 2015•journals.sagepub.com* 38, 317–349 (2015).
36. Stanish, K. D., Hooton, R. D. & Thomas, M. D. A. Testing the Chloride Penetration Resistance of Concrete: A Literature Review. https://doi.org/10.21949/1503647 (2001) doi:10.21949/1503647.
37.Chakir A, Andry JF, Ullah A, Bansal R, Ghazouani M, editors. Engineering applications of artificial intelligence. Cham: Springer Nature; 2024.
38.McCormick ME. Ocean engineering mechanics: with applications. Cambridge: Cambridge University Press; 2009.
39.Wang Q, Zhao G, Tian J. Exploring the multiscale structure of urban waterlogging resilience systems for adaptive policy optimisation. Sci Rep. 2025.
40.Behradfar A, Castanho RA. Addressing challenges and long-term visions of climate change policies in resilience-based urban planning for peripheral regions. In: Integrated Planning for Sustainable Resilient Regions. Amsterdam: Elsevier; 2025. p. 235-51.
41.Shan R, Jia X, Su X, Xu Q, Ning H, Zhang J. AI-driven multi-objective optimization and decision-making for urban building energy retrofit: advances, challenges, and systematic review. Appl Sci. 2025;15(16):8944.
42.Fleming PJ, Fonseca CM. Genetic algorithms in control systems engineering. IFAC Proc Vol. 1993;26(2):605-12.
43.Cheng FY, Li D. Multiobjective optimization design with Pareto genetic algorithm. J Struct Eng. 1997;123(9):1252-61.
44.H, Akani CB. Flood resilience, architectural design and housing development in Port-Harcourt metropolis. 2025.
45.Mabrouk M, Han H, Mahran MGN, Abdrabo KI, Yousry A. Revisiting urban resilience: a systematic review of multiple-scale urban form indicators in flood resilience assessment. Sustainability. 2024;16(12):5076.

46.Fung, J. F., Sattar, S., Butry, D. T., & McCabe, S. L. (2021). The total costs of seismic retrofits: State of the art. Earthquake Spectra, 37(4), 2991-3014.

47.Lian S, Meng T, Zhao Y, Liu Z, Zhou X, Ruan S. Experimental and theoretical analyses of chloride transport in recycled concrete subjected to a cyclic drying-wetting environment. Structures. 2023;52:1020-34.

Publisher's note Springer Nature remains neutral with regard to jurisdictional claims in published maps and institutional affiliations.

Graphical Abstract

